METHODS

Specimens. Primary tumour specimens were obtained from patients who were diagnosed with DLBCL, follicular lymphoma, MCL, MALT lymphoma, or classical Hodgkin's lymphoma. In total, 238 primary lymphoma specimens listed in Supplementary Table 1 were subjected to SNP array analysis. Three Hodgkin's-lymphoma-derived cell lines (KM-H2, HDLM2, L540) were obtained from Hayashibara Biochemical Laboratories, Inc., Fujisaki Cell Center and were also analysed by SNP array analysis.

Microarray analysis. High-molecular-mass DNA was isolated from tumour specimens and subjected to SNP array analysis using GeneChip Mapping 50K and/or 250K arrays (Affymetrix). The scanned array images were processed with Gene Chip Operation software (GCOS), followed by SNP calls using GTYPE. Genome-wide copy number measurements and LOH detection were performed using CNAG/AsCNAR software[12,13].

Mutation analysis. Mutations in the *A20* gene were examined in 265 samples of B-lineage lymphoma, including 62 DLBCLs, 52 follicular lymphomas, 87 MALTs, 37 MCLs and 3 Hodgkin's-lymphoma-derived cell lines and 24 primary Hodgkin's lymphoma samples, by direct sequencing using an ABI PRISM 3130xl Genetic Analyser (Applied Biosystems). To analyse primary Hodgkin's lymphoma samples in which CD30-positive tumour cells (Reed–Sternberg cells) account for only a fraction of the specimen, 150 Reed–Sternberg cells were collected for each 10 μm slice of a formalin-fixed block immunostained for CD30 by laser-capture microdissection (ASLMD6000, Leica), followed by genomic DNA extraction using QIAamp DNA Micro kit (Qiagen). The primer sets used in this study are listed in Supplementary Table 6.

Functional analysis of wild-type and mutant A20. Full-length cDNA for wild-type *A20* was isolated from total RNA extracted from an acute myeloid leukaemia-derived cell line, CTS, and subcloned into a lentivirus vector (pLenti4/TO/V5-DEST, Invitrogen). cDNAs for mutant A20 were generated by PCR amplification using mutagenic primers (Supplementary Table 6), and introduced into the same lentivirus vector. Forty-eight hours after transfection of each plasmid into 293FT cells using the calcium phosphate method, lentivirus stocks were obtained from ultrafiltration using Amicon Ultra (Millipore), and used to infect KM-H2 cells to generate stable transfectants of mock, wild-type and mutant A20. Each KM-H2 derivative cell line was further transduced stably with a reporter plasmid (pGL4.32, Promega) containing a luciferase gene under an NF-κB-responsive element by electroporation using Nucleofector reagents (Amaxa).

Assays for cell proliferation and NF-κB activity. Proliferation of the KM-H2 derivative cell lines was assayed in triplicate using a Cell Counting Kit (Dojindo). The mean absorption of five independent assays was plotted with s.d. for each derivative line. Two independent KM-H2-derived cell lines were used for each experiment. The NF-κB activity in KM-H2 derivatives for A20 mutants was evaluated by luciferase assays using a PiccaGene Luciferase Assay Kit (TOYO B-Net Co.). Each assay was performed in triplicate and the mean absorption of five independent experiments was plotted with s.d.

Western blot analyses. Polyclonal anti-sera against N-terminal (anti-A20N) and C-terminal (anti-A20C) A20 peptides were generated by immunizing rabbits with these peptides (LSNMRKAVKIRERTPEDIC for anti-A20N and CFQFKQMYG for anti-A20C, respectively). Total cell lysates from KM-H2 cells were separated on 7.5% polyacrylamide gel and subjected to western blot analysis using antibodies to A20 (anti-A20N and anti-A20C), IκBα (sc-847), IκBβ (sc-945), IκBγ (sc-7155) and actin (sc-8432) (Santa Cruz Biotechnology).

Functional analyses of wild-type and mutant A20. Each KM-H2 derivative cell line stably transduced with various *Tet*-inducible A20 constructs was cultured in serum-free medium in the presence or absence of A20 induction using 1 μg ml^{-1} of tetracycline, and cell number was counted every day. 1×10^6 cells of each KM-H2 derivative cell line were analysed for their intracellular levels of IκBβ and IκBε and for NF-κB activities by western blot analyses and luciferase assays, respectively, 12 h after the beginning of cell culture. Effects of human recombinant TNF-α and lymphotoxin-α (210-TA and 211-TB, respectively, R&D Systems) on the NF-κB pathway and cell proliferation were evaluated by adding both cytokines into 10 ml of serum-free cell culture at a concentration of 200 pg ml^{-1}. For cell proliferation assays, culture medium was half replaced every 12 h to minimize the side-effects of autocrine cytokines. Intracellular levels of IκBβ, IκBε and NF-κB were examined 12 h after the beginning of the cell culture. To evaluate the effect of neutralizing TNF-α and lymphotoxin-α, 1×10^6 of KM-H2 cells transduced with both *Tet*-inducible A20 and the NF-κB-luciferase reporter were pre-cultured in serum-free media for 36 h, and thereafter neutralizing antibodies against TNF-α (MAB210, R&D Systems) and/or lymphotoxin-α (AF-211-NA, R&D Systems) were added to the media at a concentration of 200 pg ml^{-1}. After the extended culture during 12 h with or without 1 μg ml^{-1} tetracycline, the intracellular levels of IκBβ and IκBε and NF-κB activities were examined by western blot analysis and luciferase assays, respectively. To examine the effects of A20 re-expression on apoptosis, 1×10^6 KM-H2 cells were cultured for 4 days in 10 ml medium with or without *Tet* induction. After staining with phycoerythrin-conjugated anti-Annexin-V (ID556422, Becton Dickinson), Annexin-V-positive cells were counted by flow cytometry at the indicated times.

***In vivo* tumorigenicity assays.** KM-H2 cells transduced with a mock or *Tet*-inducible wild-type *A20* gene were inoculated into NOG mice and their tumorigenicity was examined for 5 weeks with or without tetracycline administration. Injections of 7×10^6 cells of each KM-H2 cell line were administered to two opposite sites in four mice. Tetracycline was administered in drinking water at a concentration of 200 μg ml^{-1}.

ELISA. Concentrations of TNF-α, lymphotoxin-α, IL-1, IL-2, IL-4, IL-6, IL-12, IL-18 and TGF-β in the culture medium were measured after 48 h using ELISA. For those cytokines detectable after 48-h culture (TNFα, LTα, and IL-6), their time course was examined further using the Quantikine ELISA kit (R&D Systems).

Statistical analysis. Significance of the difference in NF-κB activity between two given groups was evaluated using a paired *t*-test, in which the data from each independent luciferase assay were paired to calculate test statistics. To evaluate the effect of A20 re-expression in KM-H2 cells on apoptosis, the difference in the fractions of Annexin-V-positive cells between Tet (+) and Tet (−) groups was also tested by a paired *t*-test for assays, in which the data from the assays performed on the same day were paired.

ELSEVIER

Experimental Hematology

Experimental Hematology 2009;37:1400–1410

Bone marrow engraftment but limited expansion of hematopoietic cells from multipotent germline stem cells derived from neonatal mouse testis

Momoko Yoshimoto[a,b], Toshio Heike[a], Hsi Chang[a], Mito Kanatsu-Shinohara[c], Shiro Baba[a], Joseph T. Varnau[b], Takashi Shinohara[c], Mervin C. Yoder[b], and Tatsutoshi Nakahata[a]

[a]*Departments of Pediatrics, Kyoto University, Kyoto, Japan;*
[b]*Department of Pediatrics, Herman B Wells Center for Pediatric Research, Indiana University School of Medicine, Indianapolis, Ind., USA;*
[c]*Molecular Genetics, Graduate School of Medicine, Kyoto University, Kyoto, Japan*

(Received 28 March 2009; revised 1 September 2009; accepted 21 September 2009)

Objective. **Multipotent germline stem (mGS) cells derived from neonatal mouse testis, similar to embryonic stem (ES) cells, differentiate into various types of somatic cells in vitro and produce teratomas after inoculation into mice. In the present work, we examined mGS cells for hematopoietic progenitor potential in vitro and in vivo.**

Materials and Methods. **mGS cells were differentiated on OP9 stromal cells and induced into $Flk1^+$ cells. $Flk1^+$ cells were sorted and replated on OP9 stromal cells with various cytokines and emerging hematopoietic cells were analyzed for lineage marker expression by fluorescein-activated cell sorting, progenitor activity by colony assay, and stem cell transplantation assay.**

Results. **mGS cells, like ES cells, produce hematopoietic progenitors, including both primitive and definitive erythromyeloid, megakaryocyte, and B- and T-cell lineages via $Flk1^+$ progenitors. When transplanted into the bone marrow (BM) of nonobese diabetic/severe combined immunodeficient (NOD/SCID) γc^{null} mice directly, mGS-derived green fluorescent protein (GFP)-positive cells were detected 4 months later in the BM and spleen. GFP^+ donor cells were also identified in the Hoechst33342 side population, a feature of hematopoietic stem cells. However, these mGS-derived hematopoietic cells did not proliferate in vivo, even after exposure to hematopoietic stressors, such as 5-fluorouracil (5FU) injection or serial transplantation.**

Conclusion. **mGS cells produced multipotent hematopoietic progenitor cells with myeloid and lymphoid lineage potential in vitro and localized in the BM after intra-BM injection but, like ES cells, failed to expand or show stem cell repopulating ability in vivo.** © **2009 ISEH - Society for Hematology and Stem Cells. Published by Elsevier Inc.**

Hematopoietic stem cells (HSCs) are defined as blood cells displaying the potential for self-renewal and multilineage differentiation. HSC transplantation has been widely used for treating hematological malignancies and inherited disorders. Peripheral blood and cord blood stem cells, as well as bone marrow cells, have been intensively studied and shown to be effective for clinical use. Recently, embryonic stem (ES) cells have been proposed as an alternative candidate source of HSCs. Many approaches have been attempted to obtain HSCs from ES cells, but this is challenging unless using enforced expression of genes, such as *Hoxb4* [1] or *Cdx4* [2] in ES cells. Even if a robust method for HSC derivation from ES cells were discovered, one would still need to address donor–host differences in histocompatibility antigens to permit ES-derived HSC engraftment in patients.

Multipotent germline stem (mGS) cells have been established from neonatal mouse testis and have been proven to have similar potential to ES cells, including germline transmission [3]. If mGS cells could be isolated from human testis and were utilized to produce HSC, then the problem of major histocompatibility complex (MHC) incompatibility would be solved because it might be possible to establish the patient's own mGS cells. In that sense, mGS cells may have a big advantage over ES cells in human application for cell therapies.

The methods for inducing hematopoietic cells from ES cells have been well-developed [4]. Flk1 is a candidate marker for mesoderm [5] and hemangioblast [6,7] cells, and Flk1 progeny have been proven to differentiate into

Offprint requests to: Momoko Yoshimoto, M.D., Ph.D., Wells Center for Pediatric Research, Indiana University School of Medicine, Indianapolis, IN 46202, USA; E-mail: myoshimo@iupui.edu

0301-472X/09 $–see front matter.
doi: 10.1016/j.exphem.2009.09.006

all hematopoietic cell lineages [8]. Using the OP9 stromal cell line as a feeder layer, hematopoietic cells are effectively induced from ES cells [9], and FLK1$^+$-derived definitive hematopoietic cells are obtained [10].

In a previous report [3], mGS cells have been shown to differentiate into CD45$^+$ hematopoietic cells, including Gr-1$^+$Mac1$^+$ myeloid cells and Ter119$^+$ erythroid cells, but the potential for mGS cells to differentiate into hematopoietic stem/progenitor has not been reported. We have observed multipotent hematopoietic progenitor cells with myeloid and lymphoid potential emerging from mGS FLK1$^+$ cells using the OP9 feeder cell system and describe the localization of mGS-derived hematopoietic cells in the bone marrow (BM) cavity when directly injected into the BM of immunodeficient mice. However, the mGS-derived hematopoietic cells present in the host, like differentiated wild-type ES-derived hematopoietic cells, do not proliferate or display multilineage repopulating ability in vivo.

Materials and methods

Cell culture

mGS cells were established from mouse neonatal testis of DBA/2 mice or a green fluorescent protein (GFP)–expressing transgenic mouse (C57BL6 x DBA/2 F1 background), as described previously [3]. The CCE ES cell line was kindly provided by Dr. S. Nishikawa (RIKEN, Kobe, Japan). The ES cell line D3 was transfected with GFP gene driven by the ubiquitous CAG promoter. These CCE and D3 cell lines are derived from the 129 mouse strain. GFP$^+$ mGS and D3 were used for the transplantation assay. The mGS or ES lines were maintained as described previously [3].

Differentiation to hematopoietic progenitor cells was induced as described [8,11]. Briefly, 10^4 of undifferentiated mGS and ES cells were seeded onto T-25 flask with confluent OP9 stromal cells (a gift from Dr. Kodama) in α–minimum essential medium supplemented with 10% fetal bovine serum and 5×10^{-5}M 2-mercaptoenthanol. After 4 days, cultured cells were harvested with cell dissociation buffer (Gibco, Grand Island, NY, USA) and Flk1$^+$ cells were collected using a FACSVantage flow cytometer (Becton Dickinson, Mountain View, CA, USA). The 5–10 $\times$ 10^3 Flk1$^+$ cells per well in six-well plate with confluent OP9 stromal cells were cocultured again with added cytokines, such as 100 ng/mL mouse stem cell factor (SCF), 10 ng/mL human thrombopoietin (TPO), 10 ng/mL mouse Flt-3 ligand (FL), 4 u/mL human erythropoietin (EPO), and 100 u/mL mouse interleukin (IL)-7. Mouse SCF, human TPO, and human EPO were kindly provided from Kirin Brewery (Tokyo, Japan). Mouse FL and IL-7 were purchased from R&D Systems (Minneapolis, MN, USA). For T-cell induction, Flk1$^+$ cells were cocultured with OP9-DL1 [12] stromal cells (kindly provided by Dr. Zuniga-Pflucker, University of Toronto) with 50 ng/mL IL-7.

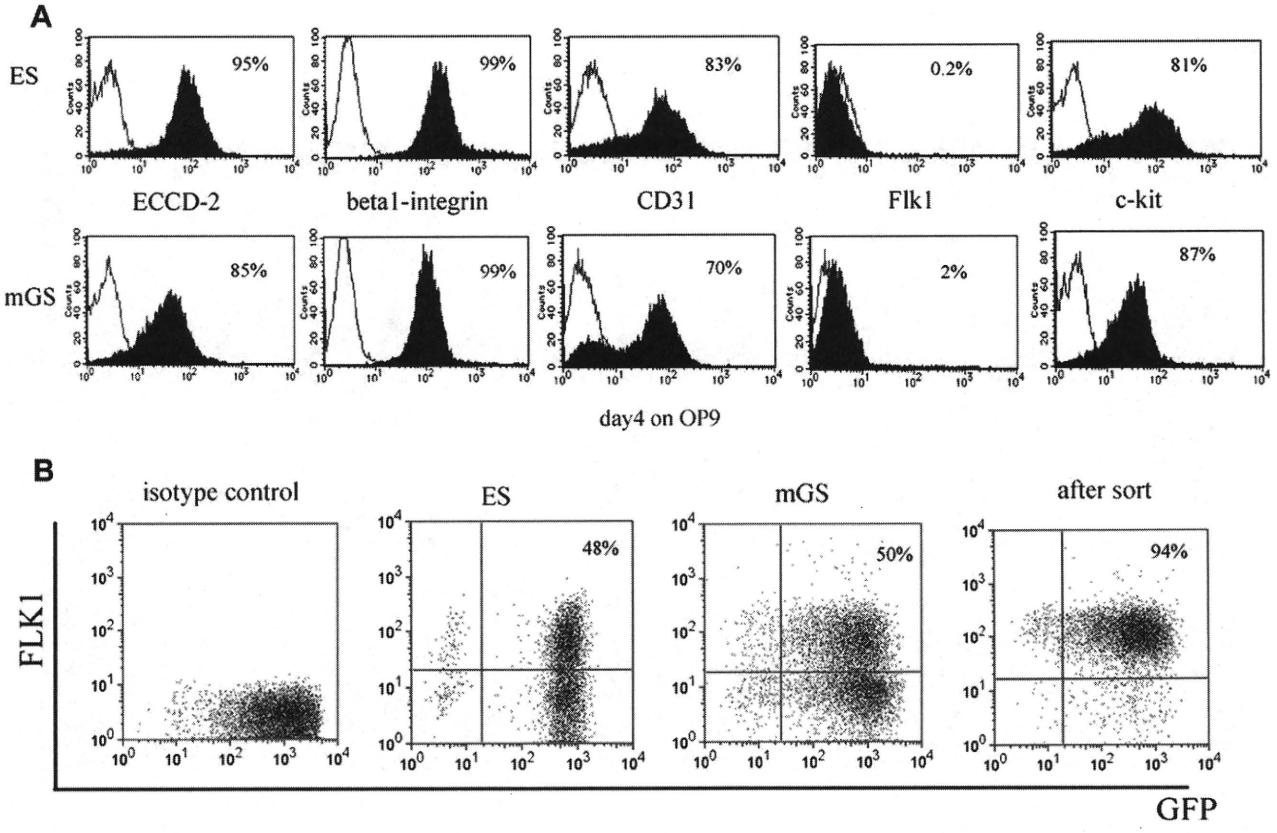

Figure 1. Surface markers of mGS and ES cells. Surface markers of undifferentiated mGS cells (**A**, lower panel) are similar to those of ES cells (**A**, upper panel). mGS cells were induced on OP9 stromal cells for 4 days and were confirmed to express Flk1 (**B**).

Hematopoietic colony-forming cell assay

In order to analyze emergence of immature hematopoietic progenitor cells from mGS cells, on each day after induction of Flk1$^+$ cells on OP9, cells were harvested and plated in methylcellulose for colony-forming assay using a modification of the technique described previously [13,14]. All cultures were performed in triplicate and the number of colony-forming cells was scored at day 8 to 10. For megakaryocyte colonies, the cells were plated in Megacult (Stem Cell Technologies, Vancouver, Canada) according to manufacturer's instruction.

Antibodies and staining

The following primary antibodies were used: rat anti-mouse E-cadherin (ECCD2, from Calbiochem. San Diego, CA, USA), fluorescein isothiocyanate (FITC)–conjugated hamster anti-rat β1 integrin (Ha2/5), rat anti-mouse CD31 (MEC 13.3), allophycocyanin (APC)-conjugated rat anti-mouse *c-kit* (2B8), phycoerythrin (PE)-conjugated rat anti-Flk1 (AVAS12), PE-conjugated rat anti-mouse Ter119 (TER-119), APC-conjugated rat anti-mouse CD45 (30-F11), biotin-conjugated rat anti-mouse Gr-1 (RB6-8C5), biotin-conjugated rat anti-mouse Mac-1 (M1/70), purified rat CD41 antibody (MWReg30), and rabbit anti-embryonic hemoglobin antibody [15] (a gift from Dr. Takakura, Osaka University). PE-conjugated or alkaline phosphatase–conjugated anti-rat IgG, APC-conjugated streptavidin, or FITC–conjugated anti-rabbit immunoglobulin G were used as secondary antibodies. All antibodies except ECCD2 were purchased from Pharmingen (San Diego, CA, USA). For detection of side population (SP) cells, BM cells were stained with Hoechst 33324, as described previously [16–18]. Stained cells were analyzed using FACSCalibur or LSRII (Becton Dickinson).

Immunohistochemistry

Femurs of recipient mice were fixed with 4% paraformaldehyde, embedded in the optimal cutting temperature compound and frozen sections of 7-μm thickness were mounted on silan-coated glass slides and were stained with rabbit anti-GFP antibody (BD Bioscience Clontech, Palo Alto, CA, USA), as described previously [19]. Cytospin preparations and culture dishes were also stained with various antibodies, as described previously [20,21].

Mice and transplantation

Nonobese diabetic/severe combined immunodeficient (NOD/SCID) γc^{null} mice were kindly provided from the Central Institute of Experimental Animals (Kawasaki, Japan) and kept under specific pathogen-free conditions in accordance with the guidelines of the facility. Cultured mGS-derived hematopoietic cells and OP9 cells were collected and injected into the femoral BM of NOD/SCIDγc^{null} mice that were irradiated with 2.4 Gy before transplantation. The 2×10^5 BM mononuclear cells were injected as a positive control. After transplantation, mice were prophylactically provided sterile water with neomycin sulfate (Gibco BRL).

For serial transplantation, BM cells were collected from transplanted NOD/SCIDγc^{null} mice 4 months after primary transplantation and stained with anti-CD45.1$^+$ (recipient) and CD45.2$^+$ (donor) antibodies. CD45.2$^+$ donor cells were sorted on FACSVantage (Becton Dickinson) and injected into the BM of 2.4-Gy irradiated NOD/SCIDγc^{null} mice. Peripheral blood (PB) and BM were analyzed 3 to 4 months after secondary transplantation.

RNA extraction and reverse transcriptase polymerase chain reaction (RT-PCR) analysis

Total RNA was prepared using Trisol (Gibco BRL). Complementary DNA (cDNA) synthesis was performed using Superscript II

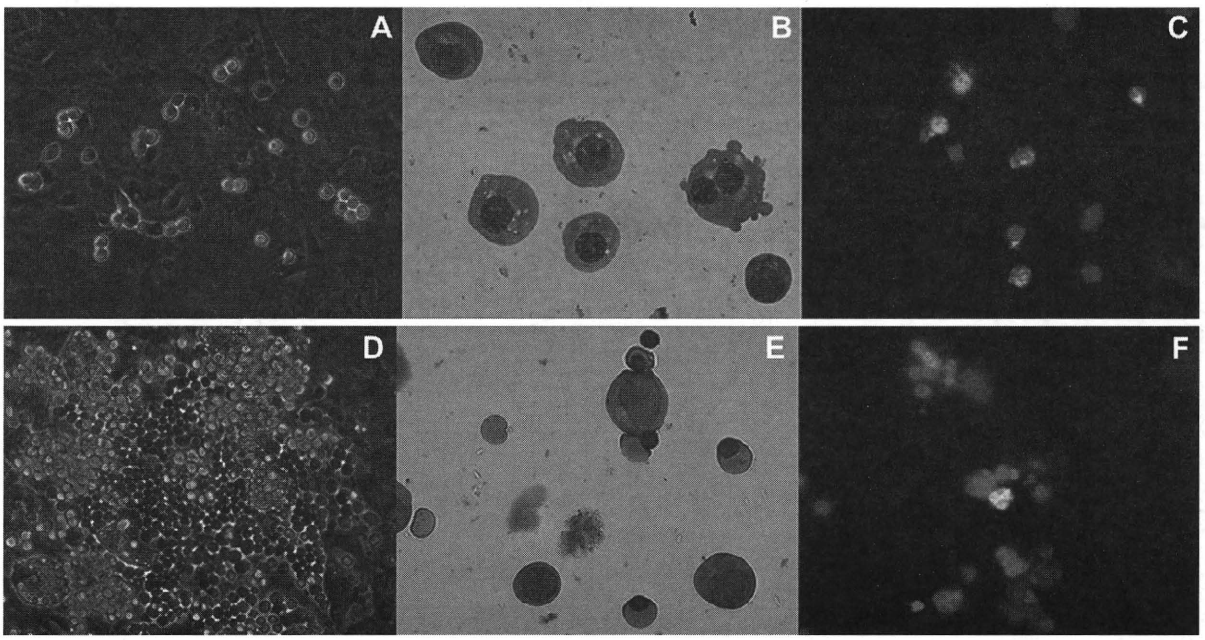

Figure 2. Primitive and definitive erythroid cells are differentiated from mGS–derived Flk1$^+$ cells. mGS-derived Flk1$^+$ cells were cultured on OP9 cells and small round cells and cobblestone-forming areas were found [(**A**) day 3, (**D**) day 9). May-Giemsa staining of a cytospin preparation [(**B**); day 3, (**E**); day 9)]. Immunostaining of E1 antigen and Ter119 (**C**,**F**). (**C**) E1 antigen; green. (**F**) E1 antigen; green Ter119; red. Nuclear staining with Hoechst 33324; blue. Magnification (**A**,**D**): ×100; (**B**,**C**,**E**,**F**): ×200.

and oligo $(dT)_{12\text{-}18}$ primers (Invitrogen, Carlsbad, CA, USA) following manufacturer's instructions. The same cDNA sample was used for PCR amplification with different primer sets, using standard protocols using AmpliTaq Gold (Applied Biosystems, Foster City, CA, USA). The primer sequences were as follows: βH1 forward: AGTCCCCATGGAGTCAAAGA, reverse: CTC AAG GAG ACC TTT GCT CA, β major forward: CTG ACA GAT GCT CTC TTG GG, reverse: CAC AAA CCC CAG AAA CAG ACA, GAPDH forward: TCC CAC TCT TCC ACC TTC, reverse: CTG TAG CCG TAT TCA TTG TC. For PCR to detect GFP, the primer sequence were as follows: GFP forward: CTG GTC GAG CTG GAC GGC GAC G, reverse: CAC GAA CTC CAG CAG GAC CAT G. Cycling parameters included: denaturation at 94°C for 30 seconds; annealing at various temperatures for 30 seconds; elongation at 72°C for 40 seconds. The number of cycle varied between 25 and 35 cycles.

Results

mGS cells can differentiate into Flk1$^+$ cells on OP9 stromal cells

It has been reported that mGS cells are very similar to ES cells in their differentiation ability into multiple cell lineages in vitro and in vivo [3]. Undifferentiated mGS and ES cells express ECCD-2, β1-integrin, CD31 and c-kit, but are negative for Flk-1 expression (Fig. 1A). In order to examine the differentiation potential of these cells, we cocultured mGS or ES cells with OP9 stromal cells and assayed for emergence of Flk1$^+$ cells 4 days after induction because Flk1 is thought to be a representative marker for mesodermal cells [5]. The percentage of Flk1$^+$ cells derived from mGS cells (50%) was very similar to ES cells (48%) (Fig. 1B).

Primitive and definitive erythropoiesis can be derived in vitro in mGS culture

In order to examine red blood cell emergence from mGS-derived Flk1$^+$ cells, Flk1$^+$ cells were sorted and cocultured on OP9 stromal cells with added EPO. Three days later, small round hematopoietic cells were found (Fig. 2A). The cytospin preparation of these cells and May-Giemsa staining revealed the round, nucleated cell morphology of primitive erythrocytes (Fig. 2B). Immunostaining with an antiembryonic hemoglobin antibody confirmed that these cells were primitive erythrocytes (Fig. 2C). After 9 days of coculture, cobblestone-forming areas were observed in

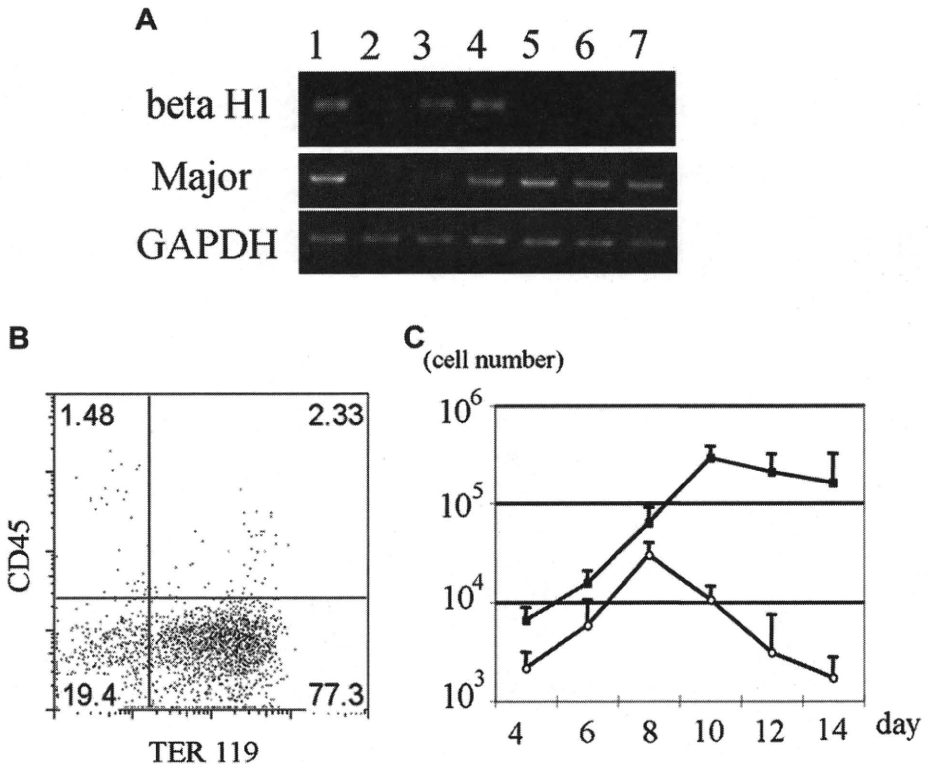

Figure 3. Erythropoiesis from mGS Flk1$^+$ cells shows two different waves. Flk1$^+$ cells were cultured on OP9 with erythropoietin (EPO) and with or without ACK45. The nonadherent cells in the culture were collected every other day, counted the number (**C**), examined the surface markers (**B**) and hemoglobin gene expression (**A**). Sequential RT-PCR analysis shows expression of β H1 hemoglobin mRNA, followed by β-major hemoglobin mRNA expression (**A**). E12.5 fetal liver (lane 1), E8.0 embryo (lane 2), mGS- Flk1$^+$ cells on OP9 for 4 days (lane 3), for 6 days (lane 4), for 8 days (lane 5), for 10 days (lane 6), for 12 days (lane 7). Flk1$^+$ cells were cultured on OP9 cells with EPO and with (white circle) or without ACK45 (black square) (**C**). Most cells in the culture were Ter119$^+$ erythrocyte (**B**). Definitive erythropoiesis was blocked by ACK45 (**C**). GAPDH = glyceraldehydes phosphate dehydrogenase.

the cultures (Fig. 2D). Morphologic analysis of nonadherent cells revealed enucleated red blood cells (Fig. 2E). Immunostaining confirmed the cells to be definitive erythrocytes that express Ter119, but not embryonic hemoglobin molecules (Fig. 2F). Next, mGS Flk1$^+$ cells were cocultured on OP9 cells in the presence of EPO or EPO and Ack45 (a blocking antibody of the c-kit signaling pathway). In this culture system, most of the emerging blood cells were Ter119$^+$ erythroid cells (Fig. 3B), but the growth factor requirements of the cultured cells in each condition showed different patterns: an initial c-kit–independent period (days 4–8; Fig. 3C) and a second c-kit–dependent period during which erythropoiesis was blocked by the presence of the Ack45 antibody (days 8–14, Fig. 3C). Erythrocytes in the initial wave expressed βH1 hemoglobin mRNA, while only β-major hemoglobin mRNA was expressed in the second wave of erythropoiesis (Fig. 3A). These results indicated that cells in the initial wave represented primitive erythrocytes, while definitive erythrocytes comprised the second wave [22]. Thus, mGS cells can give rise to primitive and definitive erythropoiesis in vitro in the same manner as differentiated ES cells.

Flk1$^+$ cells derived from mGS cell can differentiate into multiple lineages including B and T cells

When mGS-derived Flk1$^+$ cells were cocultured on OP9 cells with added SCF, granulocyte colony-stimulating factor (G-CSF), IL-3, and EPO, Flk1$^+$ cells can also differentiate into Mac1$^+$Gr1$^+$ cells and Ter119$^+$ cells (7.3% and 20.9%, respectively) similar to ES cells (7.6% and 24.3%, respectively) (Fig. 4A). Furthermore, mGS-derived Flk1$^+$ cells also gave rise to CD19$^+$ B cells and CD4$^+$CD8$^+$ T cells when cultured on OP9 cells or OP9-DL1 cells with added IL7 (Fig. 4C and D).

Flk1$^+$ cells derived from mGS cell can differentiate into multipotent progenitors

To determine whether mGS cells can give rise to clonogenic hematopoietic progenitors, Flk1$^+$ cells derived from mGS cells were cocultured on OP9 cells and all the cells after 4 to 10 days culture were plated in methylcellulose with added growth factors. Burst-forming unit-erythroid (BFU-E), colony-forming unit granulocyte-macrophage (CFU-GM), and CFU-Mix were observed (Fig. 5Aa–d). Interestingly, the number of CFU-mix was decreased after 8 days' coculture (Fig. 5Ba), and CFU-GM was the main

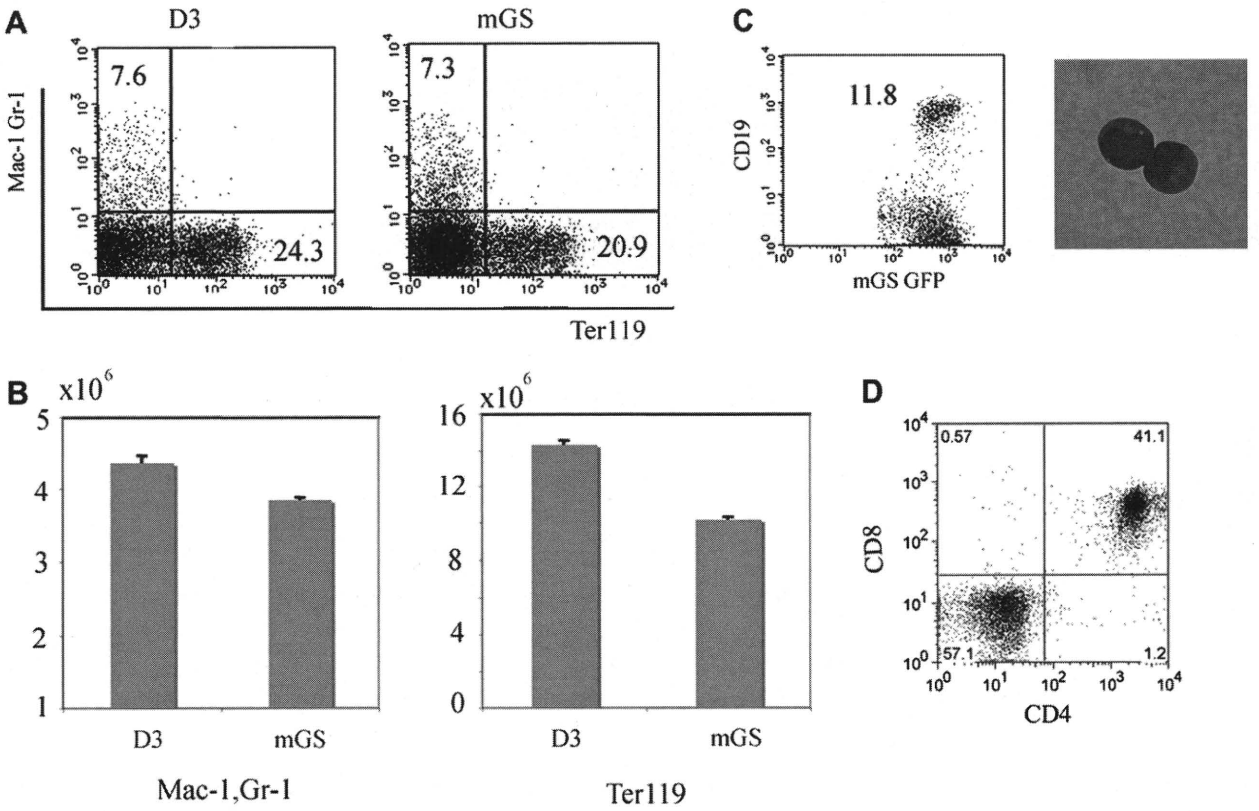

Figure 4. Myelolymphoid potential of mGS cells. Mac1$^+$Gr1$^+$, Ter119$^+$, CD19$^+$, and CD4$^+$CD8$^+$ cells were differentiated from mGS-derived Flk-1$^+$ cells within OP9 culture (**A**,**B**,**C**) or OP9-DL1 culture (**D**). For Mac1$^+$Gr1$^+$, Ter119$^+$ cells, cells were collected from 8–10 days culture (**A**,**B**). The numbers of myeloid and erythroid cells differentiated from mGS and ES cells were similar (**B**). For CD19$^+$ (**C**), and CD4$^+$CD8$^+$ cells (**D**), cells were collected from 14–21 days culture. These FACS data are representative among three independent experiments.

population detectable after 10 day's culture of mGS cells on OP9 cells. To examine whether production of these clonogenic progenitors from Flk1$^+$ cells was influenced by cytokines, Flk1$^+$ cells were cocultured on OP9 cells with only EPO or with SCF, TPO, and FL. The numbers of all kind of colonies were increased when cocultured with SCF, TPO, and FL (Fig. 5Bb). Thus, mGS-derived Flk1$^+$ cells generate multipotent hematopoietic progenitors, and this effect was promoted by addition of multiple cytokines, similar to differentiated ES cells.

Megakaryopoiesis through Flk1$^+$ cells derived from mGS cells

We also evaluated megakaryocyte production from mGS-derived Flk1$^+$ cells. Eight days after Flk1$^+$ cells were cocultured on OP9 cells in the presence of TPO and SCF, large round cells with proplatelets were observed (Fig. 5Ca). These cells expressed the cell surface protein CD41, a well-recognized marker of the platelet lineage (Fig. 5Cb). Cytospin preparations of culture fluid from these culture dishes showed large multinucleated cells that were CD41-positive (Fig. 5Cc and Cd). These cells contained both CFU-megakaryocyte and CFU-mega-mix confirmed by specific megakaryocyte progenitor cultures (Fig. 5Ce and Cf). CFU-megakaryocyte progenitors were maintained during culturing between day 8 and day 12 of mGS-derived Flk1$^+$ cells in the presence of TPO and SCF (Fig. 5D). Differentiated ES cells also showed similar trends of megakaryocyte colony production (data not shown). Thus, Flk1$^+$ cells derived from mGS cells were shown to produce megakaryocytes as well as megakaryocyte progenitor cells.

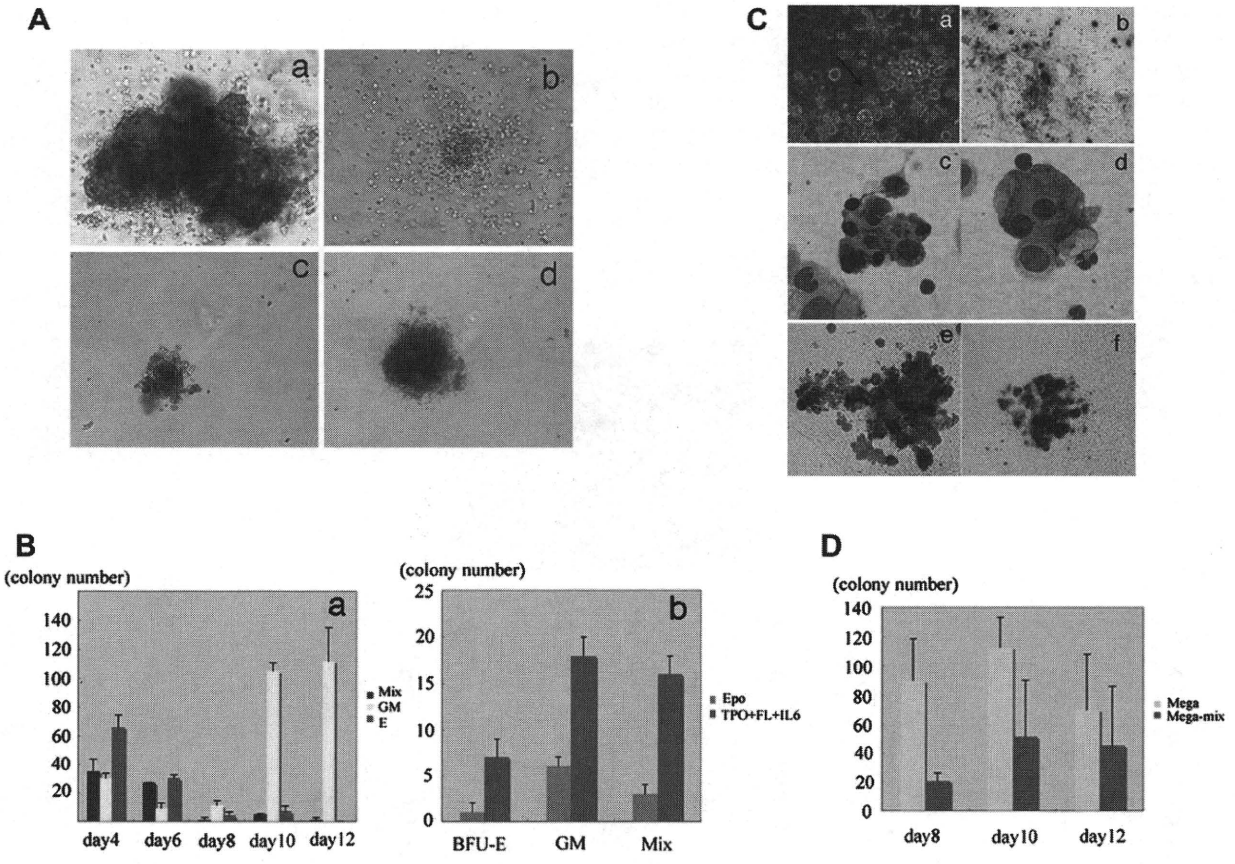

Figure 5. Colony-forming ability and megakaryocyte potential of mGS Flk1$^+$-derived cells. mGS-derived Flk-1$^+$ cells produce hematopoietic progenitor cells that can form various kinds of colonies [(**Aa**) mixed colony, (**Ab**) granulocyte-macrophage (GM) colony, (**Ac**) burst-forming unit erythroid (BFU-E), (**Ad**) mast cell colony]. Mixed colonies were predominant when mGS-derived Flk1$^+$ cells were cultured on OP9 cells for 4 to 6 days (**Ba**). Blue bar: mixed colony, yellow bar: GM colony, red bar: Erythroid colony. The number of all kinds of colonies was increased when mGS Flk1$^+$ cells were cultured on OP9 with thrombopoietin (TPO) and interleukin (IL)-6 (**Bb**). Blue bar: with erythropoietin (EPO), red bar: with TPO and IL6. Megakaryocyte or proplatelet mGS-derived Flk1$^+$ cells were observed within OP9 culture for 8–12 days. Proplatelet like cells (arrow **Ca**), Immunostaining of cultured cells with CD41 antibody secondary detected by alkaline phosphatase–conjugated antibody (**Cb** blue). Immunostaining of a cytospin preparation with CD41 antibody secondary detected by peroxidase conjugated antibody (**Cc**, **Cd** brown). After transferring cultured cells into Megacult conditions, megakaryocyte colonies (**Cf**) include mega-mix colonies (**Ce**) were found. These cells expressed acethylcholinestrase as evidenced by brown staining. The CFU-Mega was maintained during culturing day 8 to 12 in the presence of TPO and stem cell factor (**D**). Yellow bar: Megakaryo-colony, red bar: Mega-Mix colony. Magnification: (**Ca, Cb**) ×100; (**Cc**, **Cd**) ×200; (**Ce**, **Cf**) ×100.

Flk1-derived hematopoietic cells can engraft in the BM of NOD/SCIDγc^{null} mice by intra-BM injection

Finally, day-6 cocultured mGS-derived Flk1$^+$ cells and OP9 cells were recovered and injected directly into the BM of NOD/SCIDγc^{null} mice (n = 4). As a positive control, 2 × 10^5 BM mononuclear cells were injected into the BM of NOD/SCIDγc^{null} mice. Every 4 weeks after transplantation, PB was analyzed for evidence of donor-cell engraftment. While the BM cells engrafted, mGS-derived cells were barely detected (<0.1%, Fig. 6A). After 7 weeks, fluorescein-activated cell sorting (FACS) analysis revealed donor mGS-derived GFP$^+$ cells in the BM, but at low chimerism of <0.1% (data not shown). PCR analysis confirmed the presence of GFP-DNA in the BM and the spleen (Fig. 6C). Four months after transplantation, a very small number of donor CD45$^+$GFP$^+$ cells were detected in the BM and the spleen by FACS analysis and confirmed by PCR (Fig. 6A, C, and D). Furthermore, when BM cells of transplanted mice were stained with Hoechst33324, GFP$^+$ cells were detected in the SP region (Fig. 6E and F). Immunostaining of the femur revealed that GFP$^+$ cells were attached to the endosteal region, where HSCs are considered to reside (Fig. 6B). Three of four transplanted mice were confirmed to display this type of "stem cell-like" engraftment (0.03% ± 0.03%). Thus, mGS-derived hematopoietic cells are found in the BM 4 months after transplantation. It is of note that no teratoma formation was observed in any of the transplanted animals.

mGS-derived hematopoietic cells did not show stem cell potential by serial transplantation

Because HSCs are enriched in the SP fraction and normally reside in the endosteal region of the BM [23–25], we speculated that hematopoietic progeny of mGS-derived Flk1$^+$ cells engrafted in the BM and remained in the stem cell fraction. In order to prove that these GFP$^+$ cells in the BM were HSCs, we hypothesized that hematopoietic stress may induce further expansion of the donor HSCs and thus, 5FU injection and serial transplantation were performed. 5FU was injected intraperitoneally at a standard dose of 100 ug/g into transplanted mice that received mGS-derived hematopoietic cells and the PB was analyzed with CD45.1 and CD45.2 antibodies every week after 5FU injection. When the blood cell count recovered, we expected donor-derived cells would increase in number in PB, however, no donor mGS-derived cells were observed (data not shown). For secondary transplantation analysis, we

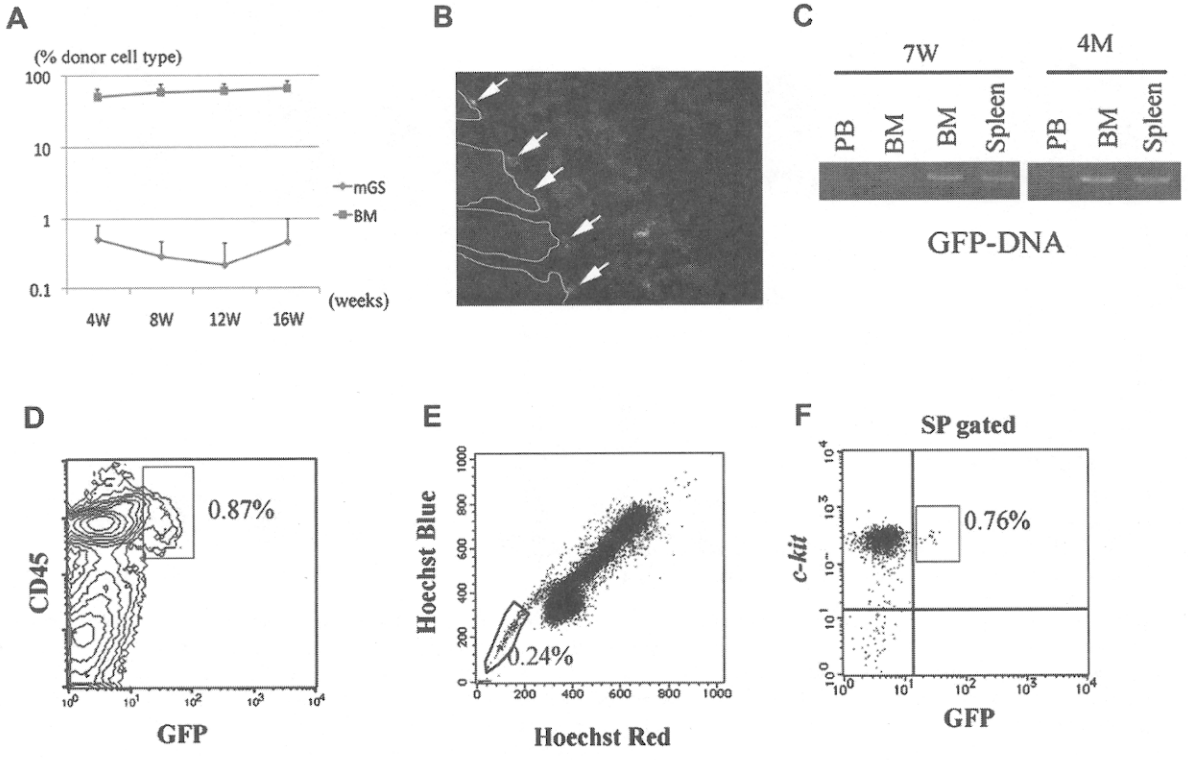

Figure 6. Transplanted hematopoietic cells from GFP$^+$ mGS cells can be detected in bone marrow (BM) 4 months after transplantation and displays stem cell phenotype. After transplantation, peripheral blood (PB) was analyzed every 4 weeks (**A**). BM cells from recipient mice 4 months after transplantation were analyzed by LSR II (**D**, **E**, **F**). GFP$^+$CD45$^+$ cells were detected (**D**). When the BM cells of the recipient mice were stained with Hoechst 33324, GFP$^+$ cells were detected in the SP region (**E**, **F**). In the section of recipient BM, GFP$^+$ cells were found attached to the endosteal region (**B**, arrow). RT-PCR shows donor-derived DNA in the BM and spleen at 7 weeks and 4 months after transplantation (**C**).

collected BM cells of primary recipient mice. Interestingly, more donor cells were detected in the lineage-negative population of the recipient BM cells (Fig. 7A) than in the whole BM (Fig. 7B). There were only 0.001% donor cells that displayed myelolymphoid lineage markers (Fig. 7B and C). Then we sorted CD45.2$^+$ mGS-derived cells from the BM of primary recipient mice (Fig. 7A) and injected 10^4 mGS-derived donor cells into the BM of irradiated secondary recipient NOD/SCIDγc^{null} mice. However, none of the host mice displayed donor-derived cells in the PB or BM after 4 months of the secondary transplantation. Thus, mGS-derived multipotent hematopoietic cells engrafted in the BM, but could not show stem cell potential by expanding and repopulating all the hematopoietic lineages posttransplantation for >16 weeks.

mGS-derived hematopoietic cells did not express CXCR4 or CDX4, but expressed HOXB4

Because mGS-derived hematopoietic cells did not engraft in the BM efficiently, we examined these cells for evidence of expression of a well-known and important homing receptor, CXCR4 (Fig. 8C). Indeed, very few mGS-derived CD45$^+$ cells expressed CXCR4. Also, c-kit expression was only 3% and the c-kit$^+$Sca-1$^+$ population represented only 0.09% of the culture elements. Because CDX4 and HOXB4 overexpression have enabled ES cells to engraft in vivo [2], the expression level of these genes was examined in mGS-derived cells using both RT-PCR and quantitative PCR. mGS-derived cells, as well as fetal liver and BM stem/progenitor cells, did not express mRNA for CDX4 (Fig. 8A). However, using the embryonic aorta-gonado-mesonephros (AGM) tissue as a reference (positive control tissue), the relative expression of HOXB4 in mGS-derived cells (0.76) was higher than embryonic day 16.5 fetal liver cells (0.02), BM lin$^-$ cells (0.09), BM Sca-1$^+$c-kit$^+$lin$^-$ cells (0.43), and CCE-derived cells (0.15) (Fig. 8B). From these results, it appears that the lack of CXCR4 expression of mGS-derived cells may be a primary reason that the transplanted cells could not expand in the recipient BM compartment.

Discussion

We report that multipotent hematopoietic progenitor cells are derived from mGS cells. mGS cells differentiate into Flk1$^+$ cells similar to differentiated ES cells. From mGS-derived Flk1$^+$ cells, erythroid, myeloid, lymphoid, and megakaryocyte hematopoietic progenitors were induced

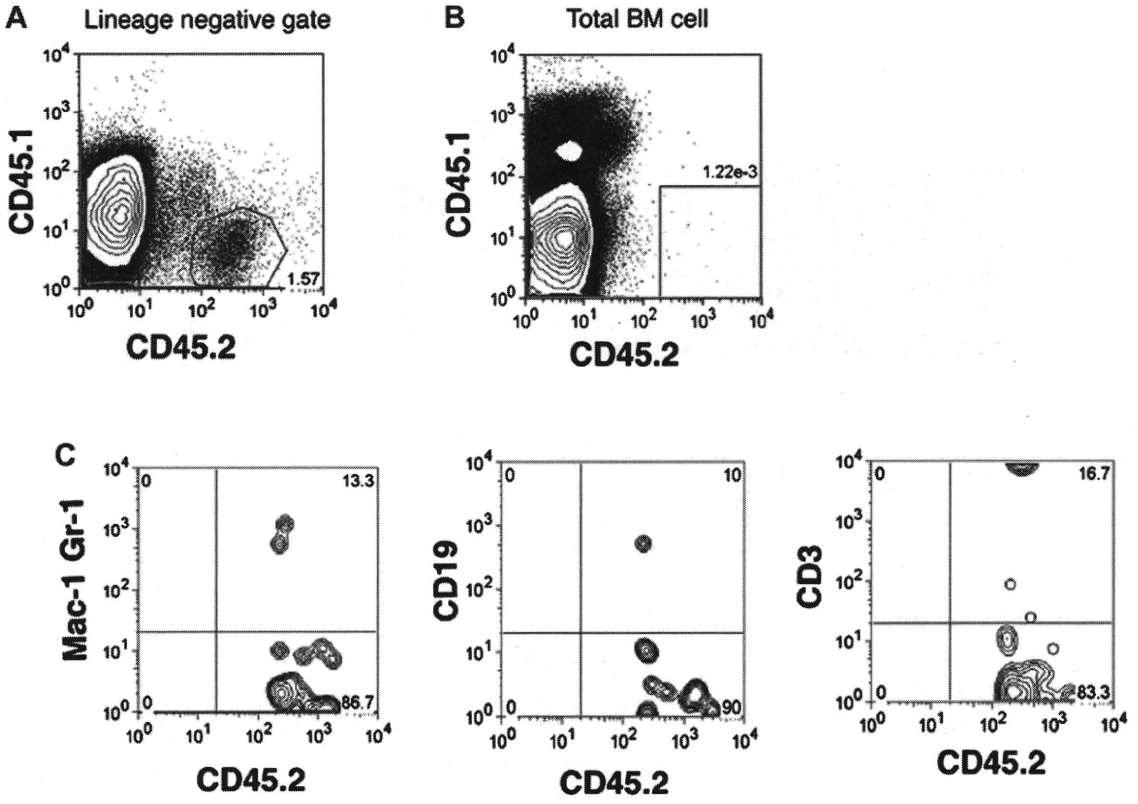

Figure 7. Analysis of primary recipient mice transplanted with mGS–derived hematopoietic cells. There are small percentages of mGS-derived cells in lineage negative fraction in the recipient bone marrow (BM) cells (**A**). When analyzing total recipient BM cells, mGS-derived cell can be detectable in very small percentage (**B**), but showed multi-lineage cell types (**C**).

efficiently in vitro in coculture with OP9 stromal cells. Furthermore, mGS-derived hematopoietic cells engrafted in the BM of NOD/SCIDγc^{null} mice, although their chimeric rate was very low. We have also transplanted hematopoietic cells differentiated from mGS-derived Flk1^{+} cells into lethally irradiated mice via tail vein, but found no significant number of donor cells in the PB or BM after transplantation (more than 30 transplanted mice, data not shown). mGS-derived cells were found in the recipient BM only when directly transplanted into the femoral BM of NOD/SCIDγc^{null} mice.

There may be several reasons why the mGS-derived Flk1^{+} progeny only engraft upon direct injection into the marrow. It is known that emergence of hematopoiesis from ES cells in vitro mirrors the emergence of hematopoiesis in the murine embryos [26]. Considering this observation, hematopoietic cells derived from mGS and ES cells should have similar characteristics to hematopoietic cells in embryos during early–mid gestation. Yolk sac cells and para-aortic splanchnopleura cells as early as E9.0 engraft in sublethally conditioned neonatal mice, but not in adult BM [27,28]. These facts lead us to speculate that mGS-derived hematopoietic cells may be too immature to express homing receptors and thus failed to find the HSC niche in the adult BM when circulating. Indeed, very few mGS-derived cells expressed CXCR4, c-kit, or Sca-1 (Fig. 8C). Furthermore, the mGS-derived Flk1^{+} progeny may fail to express high levels of human leukocyte antigen (HLA) and thus are trapped by host natural killer (NK) cells. However, NOD/SCIDγc^{null} mice have no NK cell activity [29,30] and are thus suitable for transplantation with embryonic HSCs that have just emerged from the aorta-gonado-mesonephros region at E10.5 [31]. Finally, we may have observed low chimerism due to the limited number of cells infused (1×10^5). Transplanting a larger number of cells might improve the chimerism. This limited proliferative ability of transplanted cells is similar to the behavior of human ES-derived cells transplanted in NOD/SCID mice [32].

It is interesting that donor mGS–derived hematopoietic cells that engrafted remained at the endosteal region, reported to be a niche for HSC, and that they were resident in the SP fraction 4 months after transplantation. However, these mGS-derived hematopoietic cells could not proliferate even after 5FU injection; a hematopoietic stress that normally recruits quiescent HSC into cycle and replenishment of the 5FU–depleted progenitor cell pool. In the secondary transplantation studies, as many as 30,000 to 40,000 cells were sorted from the BM of the primary recipients and injected into secondary recipient BM, and no donor cells were observed. While the most quiescent

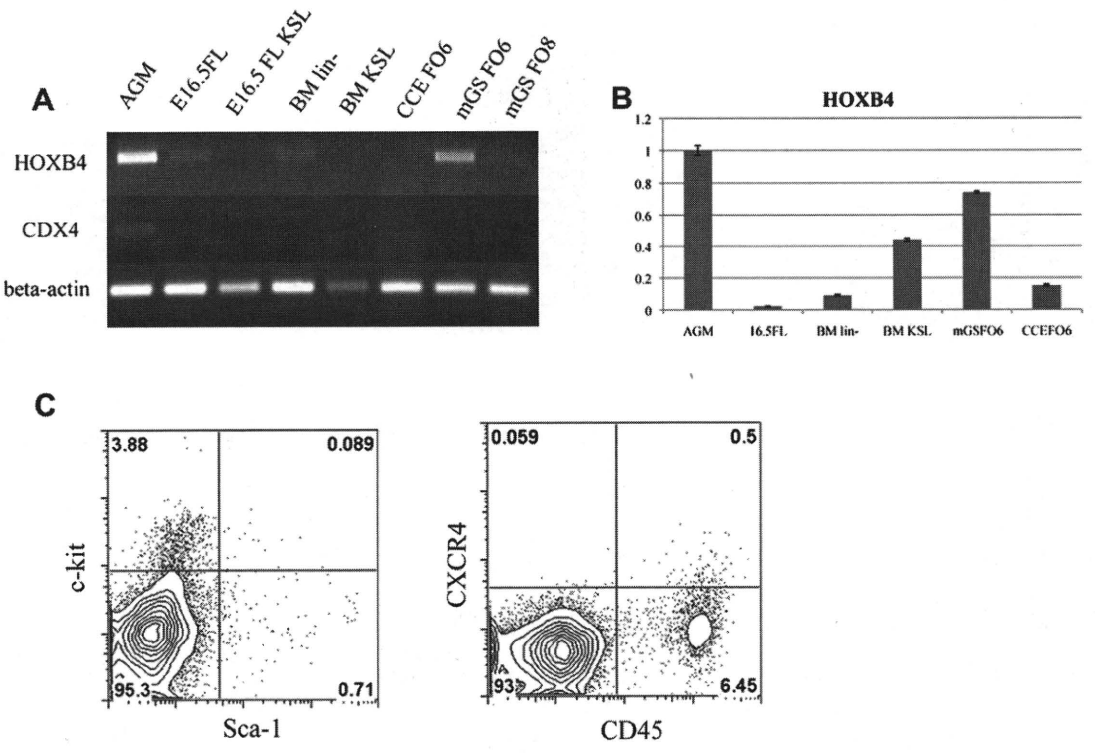

Figure 8. mGS–derived cells express HOXB4, but not CDX4 or CXCR4. RT-PCR for CDX4 and HOXB4 among various hematopoitic cells (**A**). KSL = c-kit^{+}Sca-1^{+}lineage^{-} cells, BM lin^{-} = bone marrow lineage-negative cells, FO6 = Flk1 culture on OP9 day 6, FO8 = Flk1 culture on OP9 day 8. Relative HOXB4 expression in the various hematopoitic cells (**B**). With AGM as a reference, the relative expressions of HOXB4 in each sample were follows; 16.5FL 0.02, BM lin^{-} 0.09, BM KSL 0.43, mGS FO6 0.74, CCE FO6 0.15. c-kit, Sca-1, and CXCR4 expression on mGS-derived cells [(**C**) 6 days culture].

dormant HSCs may divide every 145 days, even dormant HSC can proliferate after 5FU injection [33]. Therefore, it is unlikely that our mGS-derived multipotent cells represent dormant HSCs.

We have also shown that mGS-derived Flk-1^+ cells could produce B- and T-lymphoid cells, as well as erythromyeloid cells, using OP9 and OP9-DL1 stromal cell line cocultures. These results were very similar to ES cell differentiation studies reported previously [12,22]. Thus, mGS cells have at least the same hematopoietic potential as ES cells in vitro and in vivo.

Wild-type ES cells fail to reconstitute mouse BM without prior genetic modification [1,2]. Considering that only CDX4- and HOX B4-expressing ES cells can engraft and proliferate in vivo, it might be possible that ES or mGS-derived hematopoietic cells originally lack the proliferation potential required for in vivo expansion following engraftment. Actually, our mGS-derived cells, as well as fetal liver and BM stem/progenitor cells, did not express CDX4 transcripts. On the other hand, mGS-derived cells did express HOXB4. Because mGS-derived cells could not expand in vivo in spite of higher HOXB4 expression than fetal liver and BM progenitors, lack of CXCR4 expression may be a primary reason for the low level of donor cell chimerism rather than lack of CDX4 expression, although the question of whether upregulating CDX4 expression may enhance repopulating ability of the transplanted mGS cells needs further study. Nevertheless, this is the first report that transplanted hematopoietic cells derived from ES-like cells (mGS or ES cells) may reside in a long-lived multipotent hematopoietic cell fraction in vivo.

Recently, multipotent germline stem cells have been established from adult mouse testis [34]. Multipotent adult germline stem cells display similar characteristics to ES cells, including contributions to various organs (even germline transmission) when injected into an early blastocyst. The multipotent adult GS cells possess an advantage over ES or embryonic germ cells because they can be stably established from the postnatal mouse. Establishing multipotent adult GS cells from human subjects should be feasible both technically and ethically. Indeed, pluripotent stem cells from adult human testis have been generated [35,36]. Additionally, induced pluripotent stem cells have been established from mouse and human somatic cells and upon differentiation induced pluripotent stem cell progeny appear to have the same potential as ES-derived cells [37–39]. Which cell source will ultimately prove most efficacious for human therapy remains fertile ground for future translational research.

Acknowledgments

This study was supported by grants for Scientific Research (S) (19109006) and Scientific Research (B) (18390298,20390296) from the Ministry of Education, Science, Technology, Sports and Culture of Japan (Tokyo, Japan), Uehara Memorial Foundation (Tokyo, Japan) and by the Riley Children's Foundation (Indianapolis, IN, USA).

Conflict of Interest Disclosure

No financial interests/relationships with financial interest relating to the topic of this article have been declared.

References

1. Kyba M, Perlingeiro RC, Daley GQ. HoxB4 confers definitive lymphoid-myeloid engraftment potential on embryonic stem cell and yolk sac hematopoietic progenitors. Cell. 2002;109:29–37.
2. Wang Y, Yates F, Naveiras O, Ernst P, Daley GQ. Embryonic stem cell-derived hematopoietic stem cells. Proc Natl Acad Sci U S A. 2005;102:19081–19086.
3. Kanatsu-Shinohara M, Inoue K, Lee J, et al. Generation of pluripotent stem cells from neonatal mouse testis. Cell. 2004;119:1001–1012.
4. Kennedy M, Firpo M, Choi K, et al. A common precursor for primitive erythropoiesis and definitive haematopoiesis. Nature. 1997;386:488–493.
5. Kataoka H, Takakura N, Nishikawa S, et al. Expressions of PDGF receptor alpha, c-Kit and Flk1 genes clustering in mouse chromosome 5 define distinct subsets of nascent mesodermal cells. Dev Growth Differ. 1997;39:729–740.
6. Shalaby F, Rossant J, Yamaguchi TP, et al. Failure of blood-island formation and vasculogenesis in Flk-1-deficient mice. Nature. 1995; 376:62–66.
7. Shalaby F, Ho J, Stanford WL, et al. A requirement for Flk1 in primitive and definitive hematopoiesis and vasculogenesis. Cell. 1997;89: 981–990.
8. Nishikawa SI, Nishikawa S, Hirashima M, Matsuyoshi N, Kodama H. Progressive lineage analysis by cell sorting and culture identifies FLK1+VE-cadherin+ cells at a diverging point of endothelial and hemopoietic lineages. Development. 1998;125:1747–1757.
9. Nakano T, Kodama H, Honjo T. Generation of lymphohematopoietic cells from embryonic stem cells in culture. Science. 1994;265:1098–1101.
10. Nishikawa SI, Nishikawa S, Kawamoto H, et al. In vitro generation of lymphohematopoietic cells from endothelial cells purified from murine embryos. Immunity. 1998;8:761–769.
11. Iida M, Heike T, Yoshimoto M, Baba S, Doi H, Nakahata T. Identification of cardiac stem cells with FLK1, CD31, and VE-cadherin expression during embryonic stem cell differentiation. FASEB J. 2005;19:371–378.
12. Schmitt TM, de Pooter RF, Gronski MA, Cho SK, Ohashi PS, Zuniga-Pflucker JC. Induction of T cell development and establishment of T cell competence from embryonic stem cells differentiated in vitro. Nat Immunol. 2004;5:410–417.
13. Nakahata T, Ogawa M. Identification in culture of a class of hemopoietic colony-forming units with extensive capability to self-renew and generate multipotential hemopoietic colonies. Proc Natl Acad Sci U S A. 1982;79:3843–3847.
14. Nakahata T, Ogawa M. Hemopoietic colony-forming cells in umbilical cord blood with extensive capability to generate mono- and multipotential hemopoietic progenitors. J Clin Invest. 1982;70:1324–1328.
15. Miwa Y, Atsumi T, Imai N, Ikawa Y. Primitive erythropoiesis of mouse teratocarcinoma stem cells PCC3/A/1 in serum-free medium. Development. 1991;111:543–549.
16. Goodell MA, Brose K, Paradis G, Conner AS, Mulligan RC. Isolation and functional properties of murine hematopoietic stem cells that are replicating in vivo. J Exp Med. 1996;183:1797–1806.
17. Tsuchiya A, Heike T, Fujino H, et al. Long-term extensive expansion of mouse hepatic stem/progenitor cells in a novel serum-free culture system. Gastroenterology. 2005;128:2089–2104.

18. Nagato M, Heike T, Kato T, et al. Prospective characterization of neural stem cells by flow cytometry analysis using a combination of surface markers. J Neurosci Res. 2005;80:456–466.
19. Yoshimoto M, Chang H, Shiota M, et al. Two different roles of purified CD45+c-Kit+Sca-1+Lin- cells after transplantation in muscles. Stem Cells. 2005;23:610–618.
20. Umeda K, Heike T, Yoshimoto M, et al. Development of primitive and definitive hematopoiesis from nonhuman primate embryonic stem cells in vitro. Development. 2004;131:1869–1879.
21. Umeda K, Heike T, Yoshimoto M, et al. Identification and characterization of hemoangiogenic progenitors during cynomolgus monkey embryonic stem cell differentiation. Stem Cells. 2006;24:1348–1358.
22. Fujimoto T, Ogawa M, Minegishi N, et al. Step-wise divergence of primitive and definitive haematopoietic and endothelial cell lineages during embryonic stem cell differentiation. Genes Cells. 2001;6: 1113–1127.
23. Yoshimoto M, Shinohara T, Heike T, Shiota M, Kanatsu-Shinohara M, Nakahata T. Direct visualization of transplanted hematopoietic cell reconstitution in intact mouse organs indicates the presence of a niche. Exp Hematol. 2003;31:733–740.
24. Arai F, Hirao A, Ohmura M, et al. Tie2/angiopoietin-1 signaling regulates hematopoietic stem cell quiescence in the bone marrow niche. Cell. 2004;118:149–161.
25. Nilsson SK, Johnston HM, Coverdale JA. Spatial localization of transplanted hemopoietic stem cells: inferences for the localization of stem cell niches. Blood. 2001;97:2293–2299.
26. Choi K. The hemangioblast: a common progenitor of hematopoietic and endothelial cells. J Hematother Stem Cell Res. 2002;11:91–101.
27. Yoder MC, Hiatt K, Dutt P, Mukherjee P, Bodine DM, Orlic D. Characterization of definitive lymphohematopoietic stem cells in the day 9 murine yolk sac. Immunity. 1997;7:335–344.
28. Yoder MC, Hiatt K, Mukherjee P. In vivo repopulating hematopoietic stem cells are present in the murine yolk sac at day 9.0 postcoitus. Proc Natl Acad Sci U S A. 1997;94:6776–6780.
29. Ito M, Hiramatsu H, Kobayashi K, et al. NOD/SCID/gamma(c)(null) mouse: an excellent recipient mouse model for engraftment of human cells. Blood. 2002;100:3175–3182.
30. Hiramatsu H, Nishikomori R, Heike T, et al. Complete reconstitution of human lymphocytes from cord blood CD34+ cells using the NOD/SCID/gammacnull mice model. Blood. 2003;102: 873–880.
31. Cumano A, Ferraz JC, Klaine M, Di Santo JP, Godin I. Intraembryonic, but not yolk sac hematopoietic precursors, isolated before circulation, provide long-term multilineage reconstitution. Immunity. 2001;15:477–485.
32. Wang L, Menendez P, Shojaei F, et al. Generation of hematopoietic repopulating cells from human embryonic stem cells independent of ectopic HOXB4 expression. J Exp Med. 2005;201:1603–1614.
33. Wilson A, Laurenti E, Oser G, et al. Hematopoietic stem cells reversibly switch from dormancy to self-renewal during homeostasis and repair. Cell. 2008;135:1118–1129.
34. Guan K, Nayernia K, Maier LS, et al. Pluripotency of spermatogonial stem cells from adult mouse testis. Nature. 2006;440: 1199–1203.
35. Conrad S, Renninger M, Hennenlotter J, et al. Generation of pluripotent stem cells from adult human testis. Nature. 2008;456:344–349.
36. Kossack N, Meneses J, Shefi S, et al. Isolation and characterization of pluripotent human spermatogonial stem cell-derived cells. Stem Cells. 2009;27:138–149.
37. Takahashi K, Tanabe K, Ohnuki M, et al. Induction of pluripotent stem cells from adult human fibroblasts by defined factors. Cell. 2007;131: 861–872.
38. Takahashi K, Yamanaka S. Induction of pluripotent stem cells from mouse embryonic and adult fibroblast cultures by defined factors. Cell. 2006;126:663–676.
39. Wernig M, Meissner A, Foreman R, et al. In vitro reprogramming of fibroblasts into a pluripotent ES-cell-like state. Nature. 2007;448: 318–324.

Pediatr Blood Cancer 2010;54:329–331

BRIEF REPORT

Successful Treatment of Refractory Donor Lymphocyte Infusion-Induced Immune-Mediated Pancytopenia with Rituximab

Itaru Kato, MD,[1] Katsutsugu Umeda, MD,[1]* Tomonari Awaya, MD,[1] Yoshihiro Yui, MD,[1] Akira Niwa, MD,[1] Hisanori Fujino, MD,[1] Hiroshi Matsubara, MD,[1] Ken-Ichiro Watanabe, MD,[1] Toshio Heike, MD,[1] Naoto Adachi, MD,[2] Fumio Endo, MD,[2] Tomoyuki Mizukami, MD,[3] Hiroyuki Nunoi, MD,[3] Tatsutoshi Nakahata, MD,[1] and Souichi Adachi, MD[1]

A 6-year-old male with chronic granulomatous disease, who was transplanted with bone marrow and exhibited increasing mixed chimerism, subsequently received two donor lymphocyte infusions (DLI). Two weeks after the second DLI, the patient developed acute graft-versus-host disease (GVHD) and progressive pancytopenia that was associated with autoantibody production. Conventional treatment did not improve the pancytopenia. However, administration of Rituximab (RTX) (375 mg/m^2/week for four consecutive weeks) resulted in a rapid resolution of the pancytopenia. The patient achieved full donor chimerism without GVHD symptoms. RTX can be valuable for managing immune-mediated cytopenias that arise after DLI and are refractory to conventional therapies. Pediatr Blood Cancer 2010;54:329–331. © 2009 Wiley-Liss, Inc.

Key words: allogeneic stem cell transplantation; antibodies; graft rejection; graft-versus-host disease; immune responses; Rituximab

INTRODUCTION

Donor leukocyte infusion (DLI) is used as an immunotherapy not only for preventing the reemergence of malignancies, but also for preventing graft rejection after allogeneic hematopoietic stem cell transplantation (hSCT) that results in the development of mixed increasing chimerism [1]. However, DLI treatment is also associated with substantial toxicity. For example, it has been shown that up to 41% of patients receiving DLI suffer from myelosuppression, which could lead to death from causes other than the underlying disease [2,3]. Like the cytopenias associated with graft-versus-host disease (GVHD), the cytopenias that can arise after DLI are conventionally treated by steroids, intravenous immunoglobulin (IVIG), and splenectomy. However, the prognosis of cases that are refractory to conventional treatments remains dismal as the treatment of such cases has not been established. Anti-CD20 antibody (Rituximab, RTX), a humanized murine monoclonal antibody that is often used to treat B-cell malignancies, has been shown to effectively treat various autoimmune diseases that arise after hSCT [4–6]. Here, we describe a patient with severe immune-mediated pancytopenia after DLI who responded well to RTX therapy.

CASE REPORT

A 4-month-old male was diagnosed with X-linked chronic granulomatous disease on the basis of his reduced NADPH oxidase levels (<5%) and the complete absence of gp91-phox. Despite prophylactic treatment with trimethoprim–sulfamethoxazole and itraconazole, and interferon-γ, he suffered repeatedly from severe bacterial and fungal infections, including multiple episodes of pulmonary aspergillosis. Therefore, allogeneic hSCT was planned, and the patient was transferred at 6 years of age to our hospital for bone marrow transplantation (BMT) from a genotypically HLA-matched, blood-type compatible unrelated donor. The HLA type of the donor and the patient was HLA-A 33/24, -B 58/52, -DR 1302/1502. The conditioning regimen included fludarabine 30 mg/m^2/day for 6 days from day −7 to −2, cyclophosphamide 30 mg/kg/day for 4 days from day −6 to −3, anti-T lymphocyte globulin 2.5 mg/kg/day for 4 days from day −6 to −3, and total body irradiation 300 cGy on day −1. To prevent GVHD, the patient received tacrolimus and short-methotrexate (day 1: 10 mg/m^2, day 3.6: 7 mg/m^2), as previously reported [7]. Subsequently, 4.8×10^8/kg mononucleated cells were infused without T-cell depletion. The patient's bone marrow (BM) was analyzed serially for chimerism by microsatellite PCR, and the presence of oxidase-positive neutrophils in the peripheral blood (PB) was determined by fluorescence-activated cell sorting using a dihydrorhodamine oxidation assay. Hematopoietic engraftment occurred rapidly. The neutrophil count exceeded 0.5×10^9/L on day 10, the reticulocyte count exceeded 10‰ on day 17, and the platelet counts did not drop below 40×10^9/L during this period. However, the donor chimerism of the patient was unstable. After the dosage of tacrolimus was reduced on day 25, grade II acute GVHD of the skin developed on day 37, which was resolved by a short course of prednisolone (PSL) treatment. Subsequently, the patient achieved full donor chimerism of BM on day 61, and the oxidase-positivity of PB neutrophils was 100% on day 82. The GVHD did not worsen after treatment with PSL and tacrolimus was discontinued on days 98 and 361, respectively.

Although the patient was asymptomatic and there were no abnormal laboratory findings, the oxidase-positivity of PB neutrophils gradually decreased to 50% and 13% on days 404 and 758,

[1]Department of Pediatrics, Graduate School of Medicine, Kyoto University, Kyoto, Japan; [2]Department of Pediatrics, Graduate School of Medicine, Kumamoto University, Kumamoto, Japan; [3]Faculty of Medicine, Department of Pediatrics, University of Miyazaki, Miyazaki, Japan

The authors declare no competing financial interests.

*Correspondence to: Katsutsugu Umeda, Department of Pediatrics, Graduate School of Medicine, Kyoto University, 54, Kawahara-cho, Shogoin, Sakyo-ku, Kyoto 606-8507, Japan.
E-mail: umeume@kuhp.kyoto-u.ac.jp

Received 1 May 2009; Accepted 10 August 2009

DOI 10.1002/pbc.22280
Published online 3 November 2009 in Wiley InterScience (www.interscience.wiley.com)

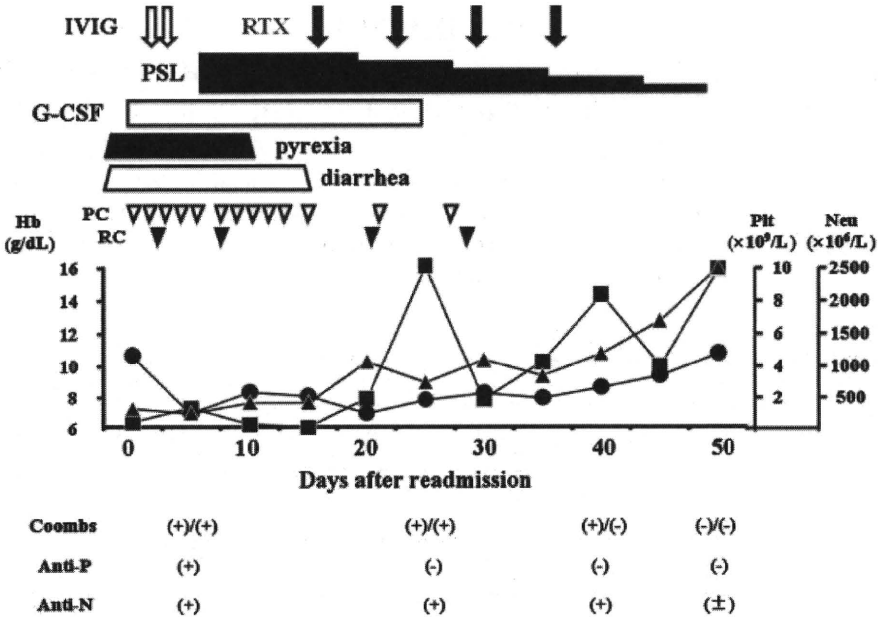

Fig. 1. The clinical course after readmission. IVIG, intravenous immunoglobulin; RTX, Rituximab; PSL, prednisolone; G-CSF, granulocyte colony-stimulating factor; RC, packed red blood cell concentrate; PC, packed platelet concentrate; Plt, platelet counts; Neu, neutrophil counts; Coombs, direct/indirect Coombs test; Anti-P, anti-platelet antibody; Anti-N, anti-neutrophil antibody. Closed circles, triangles, and squares indicate Hb levels, platelet counts (Plt), and neutrophil counts (Neu), respectively.

respectively. In an attempt to induce his return to full donor chimerism, the patient was given frozen 1.0×10^7 and 5.0×10^7 PB lymphocytes/kg on days 805 and 850, respectively, which had been harvested from the same donor who had provided the BM. Before this second DLI, the patient had not undergone any notable events such as contracting an infectious disease, medication changes or vaccinations. The clinical course after the second DLI is shown in Figure 1. Two weeks after it was delivered, the patient developed a skin rash, diarrhea, fever, elevated serum liver enzyme value, and thrombocytopenia. The patient was diagnosed clinically as having GVHD. Since restarting the patient on tacrolimus did not improve his symptoms, he was readmitted to our hospital on day 44 after the second DLI.

On readmission, the physical examination revealed no abnormal symptoms except for a persistent high fever. The results of the laboratory investigations are shown in Table I. Antibody screening tests revealed strong positivity in the direct and indirect Coombs test, and the presence of anti-platelet antibodies and anti-neutrophil antibodies specific for HNA-1a and 1b. However, other antibody screening tests were negative. There was no fungal infection or recurrence of CMV and EBV. An examination of the BM on day 896 after the BMT revealed a hypocellular marrow, but no

TABLE I. Laboratory Data on Readmission

	Value	Unit	Normal range		Value	Unit	Normal range		Value	Normal range
WBC	3.1	10^9/L	3.6–9.8	AST	38	IU/L	13–33	CMVpp65	(−)	(−)
Neu	0.93	10^9/L	1.6–6.0	ALT	36	IU/L	8–42	EBV-DNAPCR	(−)	(−)
Lymph	2.2	10^9/L	1.1–3.9	LDH	273	IU/L	129–241	Aspergillus-Ag	(−)	(−)
Hb	10.6	g/dl	11.3–13.7	ALP	473	IU/L	115–359	Candida-Ag	(−)	(−)
Reti	7.1	10^9/L	2.7–9.3	T.Bil	0.8	mg/dl	0.3–1.3	Direct Coombs Test	(+)	(−)
Plt	12	10^9/L	192–456	TP	7.3	mg/dl	6.3–8.1	Indirect Coombs Test	(+)	(−)
Haptoglobin	102.4	mg/dl	14–294	Alb	4.3	mg/dl	3.9–5.1			
CRP	4.9	mg/dl	<0.2	Soluble IL2	972	U/ml	145–519	Anti-neutrophil antibodies	(+)	(−)
β-DG	7.473	ng/ml	<11	Ferritin	7.3	ng/ml	<155	Anti-HNA-a	(+)	(−)
Endotoxin	<1.76	pg/ml	<5	Triglycerides	58	mg/dl	34–173	Anti-HNA-b	(+)	(−)
								Anti-platelet antibodies	(+)	(−)

WBC, white blood cell; Neu, neutrophil; Lymph, lymphocyte; Hb, hemoglobin; Reti, reticulocyte; Plt, platelet; CRP, C-reactive protein; β-DG, β-D-glucan; AST, aspartate aminotransferase; ALT, alanine aminotransferase; LDH, lactate dehydrogenase; ALP, alkaline phosphatase; T.Bil, total bilirubin; TP, total protein; Alb, albumin; CMVpp65, Cytomegalovirus pp65; EBV, Epstein–Barr virus; Ag, antigen; HNA, human neutrophil antigen.

evidence of malignancy or hemophagocytosis. Chimerism studies of the BM revealed 55% of the cells were composed of donor cells. Only 17% of the PB neutrophils were oxidase-positive. The patient was first treated with IVIG (1 g/kg/day for 2 days), PSL (2 mg/kg/day daily), and granulocyte colony-stimulating factor (G-CSF). Although this initial treatment resolved the pyrexia and diarrhea, the patient's pancytopenia gradually progressed and multiple transfusions became necessary. Given his refractory autoimmune pancytopenia, he was treated with RTX (375 mg/m^2/week for four consecutive weeks). The neutrophil counts rose markedly within a few days after the first RTX infusion, which was followed by the gradual increase in Hb and platelet counts. The patient became transfusion-independent after the third RTX course, and pancytopenia did not recur when the patient stopped receiving G-CSF and PSL. The hematological values normalized 21 days after the initial RTX infusion. The autoimmune antibody levels dropped during RTX treatment and eventually disappeared almost completely. Both BM chimerism studies and analysis of the oxidase-positivity of the PB neutrophils revealed 100% donor chimerism 80 days after the initial RTX infusion. Three years after the RTX treatment, the patient was alive and free of disease and showed no signs of mixed chimerism or GVHD.

DISCUSSION

Cytopenias that follow allogeneic hSCT can be immune-mediated and are frequently associated with GVHD. Autoimmune hemolytic anemia (AIHA) and immune thrombocytopenia (ITP) occur frequently, but immune-mediated cytopenias, including autoimmune neutropenia (AIN), are relatively rare [4,5]. Cytopenias are also often seen in patients after DLI and are thought to be mediated by autoimmune mechanisms, as with GVHD. In our case, pancytopenia developed soon after DLI, along with acute GVHD and the emergence of autoantibodies against multilineage blood cells. Notably, the levels of these antibodies decreased in parallel with the improvement of the pancytopenia, while the blood and BM analyses suggested that other possible causes of cytopenias, such as viral infections and hemophagocytic histiocytosis, were unlikely. However, the BM examination also showed a hypocellular marrow, which suggested that the pancytopenia did not arise from antibody-mediated cell destruction alone. Our findings suggest that autoimmunity was the major cause of the severe pancytopenia exhibited by our patient.

Most patients with autoimmune cytopenias are rescued by the administration of high-dose IVIG and standard immunosuppressive agents such as steroids [8,9]. Furthermore, RTX has been demonstrated to be useful for treating the AIHA and ITP that follow GVHD, which is refractory to conventional treatment [5,6,10–13]. However, the prognosis of patients who develop autoimmune pancytopenia remains to be determined. Page et al. [4] reported two cases that developed pancytopenia after umbilical cord blood transplantation. Despite receiving immunosuppressive treatment, including RTX, one patient continued to need the therapy while the other required a second transplantation because of pancytopenia.

Despite the fact that our patient was initially treated with PSL, high-dose IVIG, and G-CSF, and showed improvements in the other symptoms of acute GVHD, his pancytopenia progressed. Given this rapid and potentially fatal progression, we chose to start a salvage therapeutic approach rather than continue such conventional treatments, which would result in a slower response. The institution of RTX resulted in the resolution of the pancytopenia and the almost complete disappearance of the autoimmune antibodies. Furthermore, the response to RTX was already obvious 1 week after the first RTX infusion, which is consistent with a study that showed that RTX induces a prompt response in a subpopulation of patients [14].

Although no definite conclusions can be drawn from a single case with a relatively short period of follow-up, this case strengthens the hypothesis that RTX can be a beneficial treatment for refractory DLI-induced immune-mediated pancytopenia. This case suggests that further clinical research examining the merits of RTX in such cases is warranted.

REFERENCES

1. Slavin S, Morecki S, Weiss L, et al. Donor lymphocyte infusion: The use alloreactive and tumor-reactive lymphocytes for immunotherapy of malignant and nonmalignant diseases in conjunction with allogeneic stem cell transplantation. J Hematother Stem Cell Res 2002;11:265–276.
2. Kolb HJ, Schattenberg A, Goldman JM, et al. Graft-versus-leukemia effect of donor lymphocyte transfusions in marrow grafted patients. Blood 1995;86:2041–2050.
3. Collins RHJR, Shpiberg O, Drobyski WR, et al. Donor leukocyte infusions in 140 patients with relapsed malignancy after allogeneic bone marrow transplantation. J Clin Oncol 1997;15:433–444.
4. Page KM, Mendizabal AM, Prasad VK, et al. Posttransplant autoimmune hemolytic anemia and other autoimmune cytopenias are increased in very young infants undergoing unrelated donor umbilical cord blood transplantation. Biol Blood Marrow Transplant 2008;14:1108–1117.
5. Raj K, Narayanan S, Auguston B, et al. Rituximab is effective in the management of refractory autoimmune cytopenias occurring after allogeneic stem cell transplantation. Bone Marrow Transplant 2005;35:299–301.
6. Zaja F, Bacigalupo A, Patriaca F, et al. Treatment of refractory chronic GVHD with rituximab: A GITMO study. Bone Marrow Transplant 2007;40:273–277.
7. Kojima S, Matsuyama T, Kato S, et al. Outcome of 154 patients with severe aplastic anemia who received transplants from unrelated donors: The Japan Marrow Donor Program. Blood 2002;100:799–803.
8. Cines DB, Bussel JB. How I treat idiopathic thrombocytopenic purpura (ITP). Blood 2005;106:2244–2251.
9. Gehrs BC, Friedberg RC. Autoimmune hemolytic anemia. Am J Hematol 2002;69:258–271.
10. Stasi R, Pagano A, Stipa E, et al. Rituximab chimeric CD20 antibody treatment for adults with chronic idiopathic thrombocytopenic purpura. Blood 2001;98:952–957.
11. Ratanatharathorn V, Carson E, Reynolds C, et al. Anti-CD20 chimeric monoclonal antibody treatment of refractory immune-mediated thrombocytopenia in a patient with chronic graft-versus-host disease. Ann Intern Med 2000;133:275–279.
12. Hongeng S, Tardong P, Worapongpaiboon S, et al. Successful treatment of refractory autoimmune hemolytic anaemia in a post-unrelated bone marrow transplant paediatric patient with Rituximab. Bone Marrow Transplant 2002;29:871–872.
13. Corti P, Bonanimi S, Vallinoto C, et al. Rituximab for immune hemolytic anaemia following T and B cell depleted hematopoietic stem cell transplantation. Acta Haematol 2003;109:43–45.
14. Mohty M, Marchetti N, El-Cheikh J, et al. Rituximab as salvage therapy for refractory chronic GVHD. Bone Marrow Transplant 2008;41:909–911.

Cell Death and Differentiation (2010), 1–10

www.nature.com/cdd

Glyoxalase-I is a novel target against Bcr-Abl$^+$ leukemic cells acquiring stem-like characteristics in a hypoxic environment

M Takeuchi[1,2], S Kimura*[,1,3], J Kuroda[4], E Ashihara[1], M Kawatani[5], H Osada[5], K Umezawa[6], E Yasui[7], M Imoto[8], T Tsuruo[9], A Yokota[1], R Tanaka[1], R Nagao[1], T Nakahata[10], Y Fujiyama[2] and T Maekawa[1]

Abl tyrosine kinase inhibitors (TKIs) such as imatinib and dasatinib are ineffective against Bcr-Abl$^+$ leukemic stem cells. Thus, the identification of novel agents that are effective in eradicating quiescent Bcr-Abl$^+$ stem cells is needed to cure leukemias caused by Bcr-Abl$^+$ cells. Human Bcr-Abl$^+$ cells engrafted in the bone marrow of immunodeficient mice survive under severe hypoxia. We generated two hypoxia-adapted (HA)-Bcr-Abl$^+$ sublines by selection in long-term hypoxic cultures (1.0% O_2). Interestingly, HA-Bcr-Abl$^+$ cells exhibited stem cell-like characteristics, including more cells in a dormant, increase of side population fraction, higher β-catenin expression, resistance to Abl TKIs, and a higher transplantation efficiency. Compared with the respective parental cells, HA-Bcr-Abl$^+$ cells had higher levels of protein and higher enzyme activity of glyoxalase-I (Glo-I), an enzyme that detoxifies methylglyoxal, a cytotoxic by-product of glycolysis. In contrast to Abl TKIs, Glo-I inhibitors were much more effective in killing HA-Bcr-Abl$^+$ cells both *in vitro* and *in vivo*. These findings indicate that Glo-I is a novel molecular target for treatment of Bcr-Abl$^+$ leukemias, and, in particular, Abl TKI-resistant quiescent Bcr-Abl$^+$ leukemic cells that have acquired stem-like characteristics in the process of adapting to a hypoxic environment.
Cell Death and Differentiation (2010) **0**, 000–000. doi:10.1038/cdd.2010.6

Chronic myeloid leukemia (CML) is a disorder of hematopoietic stem cells caused by the constitutive activation of the Bcr-Abl tyrosine kinase.[1] Treatment of CML has been drastically improved by the development of imatinib mesylate, an Abl tyrosine kinase inhibitor (TKI).[2,3] However, imatinib resistance is frequently observed, especially in patients with advanced-stage disease.[4] Second-generation Abl TKIs, such as dasatinib,[5] nilotinib[6] and INNO-406 (formerly NS-187),[7–9] potently overcome most imatinib resistance mechanisms.[10] However, whether TKI alone can kill all the cancerous cells, which is a prerequisite for curing CML, is in doubt because TKIs are much less effective against quiescent CML stem cells.[11,12]

Bone marrow (BM) is a hypoxic tissue, particularly at the epiphysis, which is distant from the BM arterial blood supply (Supplementary Figure 1).[13] In addition, leukemic cells are more hypoxic than normal cells in the BM because of cell crowding, due to accelerated cell growth, as well as the anemia that commonly accompanies the progression of leukemia.[14,15] The oxygen supply is frequently inadequate for the level of oxygen consumption in the microenvironment of rapidly proliferating cancer cells.[16] Although not identified conclusively until today, Bcr-Abl$^+$ CML stem cells are in a quiescent state in the niche. In addition, human primary leukemic cells expressing CD34 inoculated into immunodeficient mice initially populate the hypoxic epiphysial region.[17] Thus, it is likely that quiescent leukemic cells predominantly reside in and survive in a hypoxic BM environment.

Most cancer cells that have adapted to hypoxia are resistant to a variety of cell death stimuli.[18,19] A shift in energy production from aerobic to anaerobic respiration causes a number of dramatic changes in cell phenotype, including the accumulation of hypoxia-specific by-products, alterations in the cell cycle, and resistance to chemotherapeutic drugs. Given these observations, we hypothesized that adaptation to hypoxia is one of the causes of minimal residual disease in patients treated with Abl TKIs. The molecular mechanisms of adaptation to hypoxia may provide new targets for cancer-specific therapies that are effective against cells in hypoxic microenvironments.[20,21]

[1]Department of Transfusion Medicine and Cell Therapy, Kyoto University Hospital, Kyoto, Japan; [2]Division of Gastroenterology and Hematology, Department of Internal Medicine, Shiga University of Medical Science, Shiga, Japan; [3]Division of Hematology, Respiratory Medicine and Oncology, Department of Internal Medicine, Faculty of Medicine, Saga University, Saga, Japan; [4]Division of Hematology and Oncology, Department of Medicine, Kyoto Prefectural University of Medicine, Kyoto, Japan; [5]Antibiotics Laboratory, Discovery Research Institute, RIKEN, Saitama, Japan; [6]Faculty of Science and Technology, Keio University, Yokohama, Japan; [7]Research Institute of Pharmaceutical Sciences, Musashino University, Tokyo, Japan; [8]Department of Biosciences and Informatics, Faculty of Science and Technology, Keio University, Yokohama, Japan; [9]Cancer Chemotherapy Center, Japanese Foundation for Cancer Research, Tokyo, Japan and [10]Department of Pediatrics, Graduate School of Medicine, Kyoto University, Kyoto, Japan

*Corresponding author: S Kimura, Division of Hematology, Respiratory Medicine and Oncology, Department of Internal Medicine, Faculty of Medicine, Saga University, 5-1-1 Nabeshima, Saga 849-8501, Japan. Tel: +81 952 342 353; Fax: +81 952 342 017; E-mail: shkimu@cc.saga-u.ac.jp

Keywords: hypoxia; leukemia; stem cell; Glo-I; Abl tyrosine kinase

Abbreviations: TKI, tyrosine kinase inhibitor; CML, chronic myeloid leukemia; BM, bone marrow; HA, hypoxia-adapted; Glo-I, glyoxalase-I; NOG, NOD/SCID/γ_c^{null}; BBGC, *S*-*p*-bromobenzyl glutathione cyclopentyl diester; COTC, 2-crotonyloxymethyl-4,5,6-trihydroxycylohex-2-enone; $\Delta\psi$m, mitochondrial transmembrane potential; $DiOC_6$, 3,3′-dihexyloxacarbocyanine iodide; ECL, enhanced chemiluminescence; PMSF, phenylmethylsulfonyl fluoride; PI, propidium iodide; PB, peripheral blood

Received 30.4.09; revised 18.12.09; accepted 05.1.10; Edited by

Journal: CDD ☐ Disk used Despatch Date: 21/1/2010 Figs 1,2,3,4 color
Article : npg_cdd_cdd20106 Pages: 1–10 OP: XXX ED: XXX CE: XXX Graphic: XXX

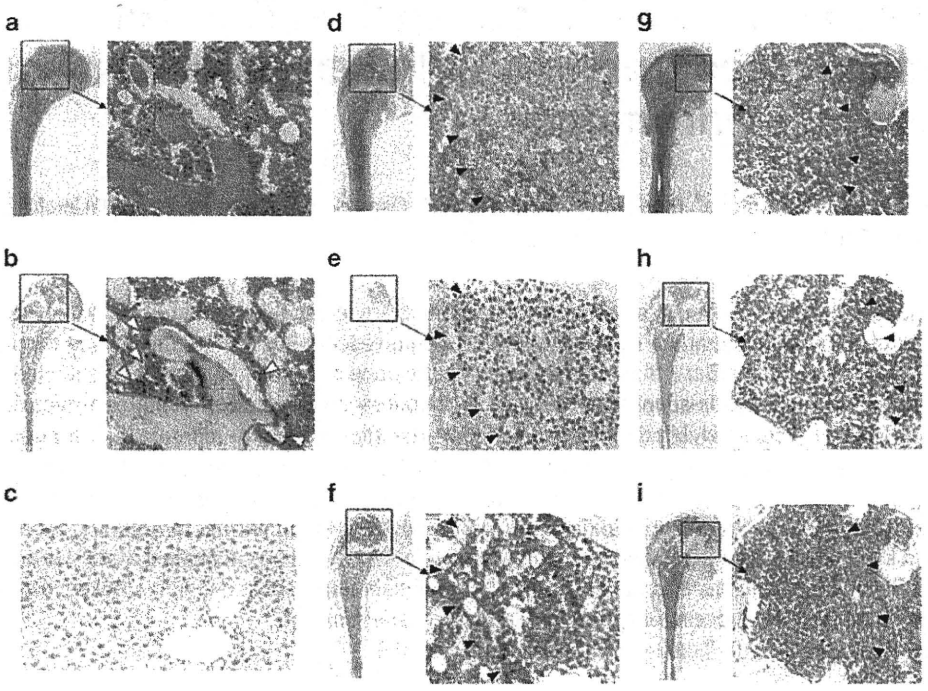

Figure 1 Engraftment of human Bcr-Abl$^+$ leukemic cells in mice. The femur of a non-engrafted mouse was stained with (**a**) hematoxylin–eosin (H&E) and (**b**) anti-pimonidazole (Ab), and the (**c**) liver was stained with anti-pimonidazole. In (**a**), the bone marrow (BM) was populated by normal mouse hematopoietic cells, and in (**b**), only a small population of normal cells was positive for pimonidazole (open triangles, Δ) along the endosteum. In (**c**), no hepatic cells were positive for pimonidazole. The femur of a K562-engrafted mouse was stained with (**d**) H&E, (**e**) antihuman Ki-67 or (**f**) anti-pimonidazole. In (**d**), the epiphysis of the bone was populated by engrafted chronic myeloid leukemia (CML) cells (closed triangles, ▲). In (**e**), the area of Ki-67-positive cells (closed triangles) was in good agreement with the area of engrafted CML cells in (**d**). Most of the engrafted CML cells were positive for Ki-67, but a few cells were negative. In (**f**), most of the engrafted CML cells (encircled by closed triangles, ▲) were positive for pimonidazole. The femur of a mouse engrafted with primary Bcr-Abl$^+$ leukemic cells from a Ph$^+$ acute lymphoblastic leukemia (Ph$^+$ ALL) patient was stained with (**g**) H&E, (**h**) antihuman Ki-67 or (**i**) anti-pimonidazole

Results

Bcr-Abl$^+$ cells in the BM survive in hypoxic conditions. Four NOD/SCID/γ_c^{null} (NOG) mice were inoculated with 1.0×10^6 K562 cells, a human cell line established from a Bcr-Abl$^+$ CML patient. Mice were killed 35 days after transplantation and examined for engraftment. Viable K562 engraftments in the BM were identified in three of the four mice. In the mouse with failed engraftment (Figure 1a), only a small population of normal cells were positive for pimonidazole, which specifically accumulates in hypoxic cells ($<1.3\%$ O_2 concentration) along the endosteum (Figure 1b). Liver cells from this were also negative for pimonidazole (Figure 1c). The transplanted K562 cells initially populated the epiphysis in recipient NOG mice. The engrafted cells were easily distinguished from normal mouse hematopoietic cells by their larger size and prominent nuclei (Figure 1d). Immunohistochemical staining with an antibody specific for human Ki-67, which is expressed in actively cycling but not quiescent cells (G_0) (Figure 1e),[22] also confirmed that K562 cells were successfully engrafted. The area of Ki-67-positive staining was in good agreement with the engraftment area estimated by cell morphology (Figures 1d and e). Although most of the engrafted cells were positive for Ki-67, a few cells were not (Supplementary Figure 2), suggesting that some engrafted K562 cells may have entered a quiescent G_0 state.[22] The majority of engrafted K562 cells were also positively labeled by pimonidazole (Figure 1f). Next, we engrafted NOD/SCID mice with primary Bcr-Abl$^+$ cells from a Ph$^+$ acute lymphoblastic leukemia (Ph$^+$ ALL) patient. Engrafted primary Bcr-Abl$^+$ cells (Figure 1g) were very similar to engrafted K562 cells (Figures 1e and f) in Ki-67 expression and pimonidazole staining (Figures 1h and i). These results indicate that both the engrafted Bcr-Abl$^+$ cell line K562 and the primary leukemic cells survive in the severely hypoxic conditions of the BM.

HA-CML cell lines. To generate hypoxia-adapted (HA)-CML cells, four CML-derived cell lines, K562, KCL22, BV173 and MYL, were continuously cultured under hypoxic conditions (1.0% O_2). Most cells were arrested in the G_1 phase of the cell cycle 2 days after transfer to hypoxic conditions as shown by an increase in the percentage of sub-G_1 cells in all four cell lines. Most of these cells underwent apoptosis within 7 days, and none of the BV173 or MYL cells survived more than 7 days (Supplementary Figure 3). In contrast, a small fraction of K562 and KCL22 cells survived in 1.0% O_2 for more than 7 days. We isolated these HA sublines of K562 and KCL22 (termed K562/HA and KCL22/HA, respectively), and these cells continued to proliferate under 1.0% O_2 for more than a year (Figures 2a and b). The

NPG.CDD.CDD20106

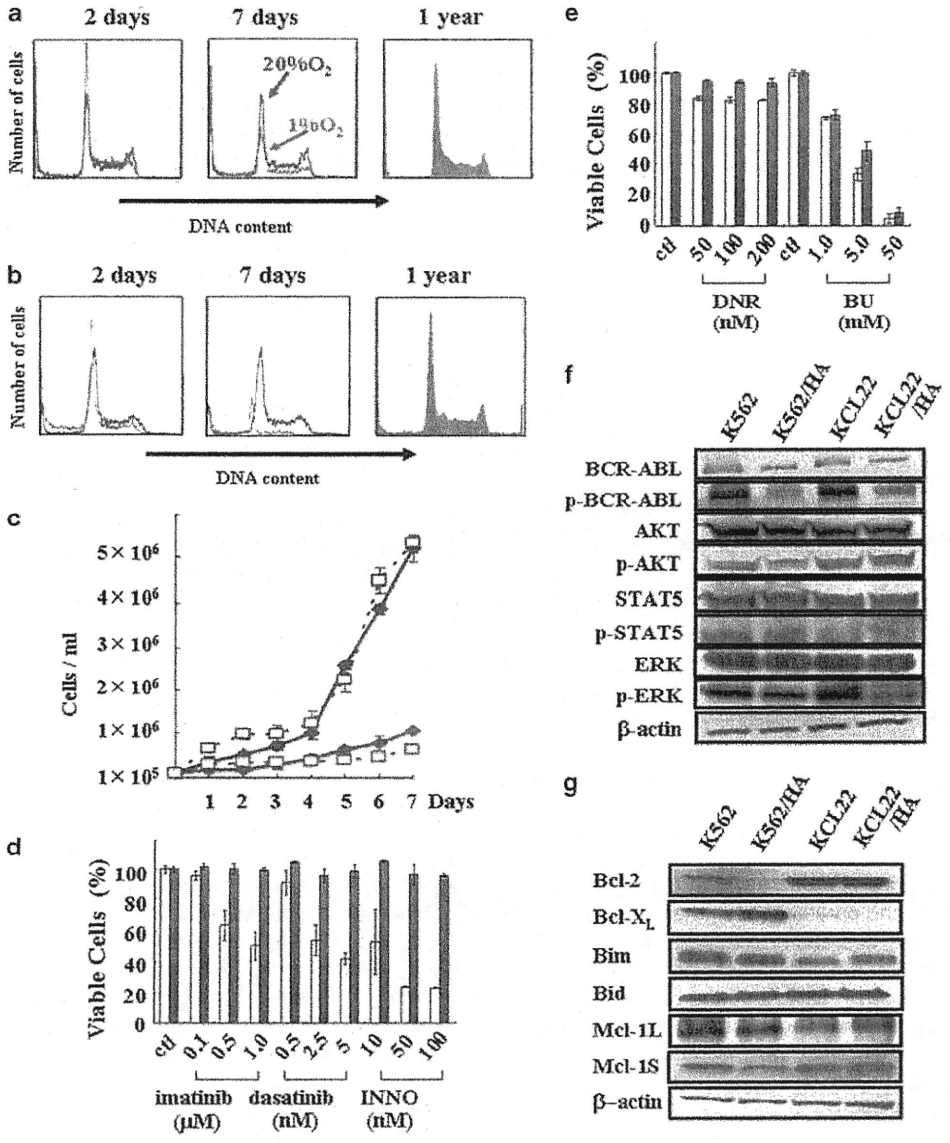

Figure 2 Characteristics of hypoxia-adapted chronic myeloid leukemia (HA-CML) cells. DNA histograms of (**a**) K562 and (**b**) KCL22 cells incubated in 1.0% O_2 (red) and 20% O_2 (blue) for 2 days, 7 days and 1 year. (**c**) Growth of K562 (blue, solid line), K562/HA (red, solid line), KCL22 (blue, broken line) and KCL22/HA (red, broken line) cells. K562 and KCL22 cells were cultured in 20% O_2, and K562/HA and KCL22/HA cells were cultured in 1.0% O_2. Antiproliferative effects of the indicated concentrations of (**d**) Abl tyrosine kinase inhibitors (TKIs) and (**e**) alkylating agents on parental K562 (white column) and K562/HA (black column) cells. (**f**) Protein expression and phosphorylation of Bcr-Abl and related kinases in parental CML cell lines and the corresponding HA subclones. (**g**) Protein levels of the indicated anti- and proapoptotic molecules in parental CML cell lines and the respective HA subclones

growth rate of both HA-CML cell lines *in vitro* was slower than that of the corresponding parental cells. Although the cell cycle distribution of both the HA cell lines was similar to that of the parental cell lines after 1 year (Figures 2a and b), the growth of the HA-CML cells was still much slower than their respective parental cell lines (Figure 2c).

We next examined the cytotoxic effects of the Abl TKIs, including imatinib, dasatinib and INNO-406, on K562, K562/HA, KCL22 and KCL22/HA cells. K562/HA cells were highly resistant to all Abl TKIs examined, compared with the parental K562 cells (Figure 2d, Table 1). As the parental KCL22 cells are intrinsically resistant to imatinib and INNO-406, we examined the antiproliferative effects of dasatinib, which has higher affinity for Abl than the other Abl TKIs, in KCL22 and KCL22/HA cells. KCL22/HA cells were approximately 50-fold less sensitive to dasatinib than the parental KCL22 cells (Table 1). Both K562/HA and KCL22/HA cells were less sensitive to the alkylating agents daunorubicin and busulfan than the respective parent cells (Figure 2e, Table 1). These results indicate that the K562/HA and KCL22/HA cells acquired resistance to a wide range of antileukemia agents during adaptation to hypoxia.

NPG.CDD.CDD20106

Table 1 IC_{50} scores of tyrosine kinase inhibitors, alkylating agents and Glo-I inhibitors for human CML cell lines and their hypoxia-adapted (HA) subclones

	K562	K562/HA	KCL22	KCL22/HA
ABL TKIs				
Imatinib (nM)	900	7400	—	—
Dasatinib (nM)	3.6	8.9	46.2	2264
INNO-406 (nM)	10.7	142.6	—	—
Alkylating agents				
Daunorubicin (nM)	—	—	105	954.3
Busulfan (mM)	2.4	4.5	2.2	3.0
Glo-I inhibitor				
BBGC (μM)	21.6	5.7	40.7	12.6
COTC (μM)	45.9	16.8	29.6	17.9
m-GFN (μM)	>300	230.2	>300	174.2

BBGC, *S-p*-bromobenzyl glutathione cyclopentyl diester; CML, chronic myeloid leukemia; COTC, 2-crotonyloxymethyl-4,5,6-trihydroxycylohex-2-enone; Glo-I, glyoxalase-I; TKI, tyrosine kinase inhibitor.

The levels of phosphorylation of Bcr-Abl and its downstream effector Erk were reduced in K562/HA and KCL22/HA cells under hypoxic conditions (1.0% O_2), compared with levels in the parental cells cultured in normoxic conditions. The levels of phosphorylated Akt (p-Akt) and Stat5 (p-Stat5) were similar in both HA and parental cells (Figure 2f). We examined the levels of apoptosis-related proteins such as Bcl-2, Bcl-xL, Bim, Bad, Mcl-1L and Mcl-1S. The levels of Bcl-2 were lower in K562/HA cells than in K562 cells, whereas the levels of Bcl-xL were higher. Bim and Bid interact with Bcl-2 and Bcl-xL to induce apoptosis. The levels of Bim and Bid in K562/HA cells were not different from those in the parental cells. The level of the antiapoptotic Mcl-1L was the same in K562/HA and parental cells, whereas the level of the proapoptotic Mcl-1S decreased in K562/HA cells (Figure 2g). In contrast to K562 and K562/HA cells, there were no differences between KCL22 and KCL22/HA cells (Figure 2g). These findings suggest that adaptation to hypoxia may have some impact on the mechanisms for executing apoptosis, although further investigation will be required to confirm this hypothesis.

Glo-I in HA-CML cells. We examined the ATP levels in parental and HA-CML cells. The amounts of ATP in K562/HA and KCL22/HA cells were 73.0 and 93.2%, respectively, of the levels in their respective parental cell lines under normoxia (Figure 3a). In addition, both HA cell lines exhibited high levels of glucose consumption and lactate production compared with their respective parental cells (Supplementary Figure 4). Normally, one molecule of glucose produces approximately 34–36 ATPs by aerobic respiration, but only 2 ATPs by glycolysis (Figure 3b). Our results suggest that anaerobic glycolysis generates sufficient ATP for survival of HA-CML cells in hypoxic conditions.

When cells preferentially use glycolysis for energy production, glycolysis-specific cytotoxic by-products, such as methylglyoxal, accumulate intracellularly. As glyoxalase-I (Glo-I) protects cells and promotes cell survival by detoxifying methylglyoxal (Figure 3b), we examined Glo-I in HA-CML cells. Both K562/HA and KCL22/HA cells had higher Glo-I protein levels (Figure 3c) and enzymatic activity (Figure 3d) than the parental cells. Furthermore, the Glo-I protein level increased markedly in the parental K562 cells after cultivation in 1.0% O_2 for 28 days (Figure 3e). In addition, we examined the Glo-I protein levels in primary Bcr-Abl $^+$ cells from CML and Ph $^+$ ALL patients. Both samples of primary Bcr-Abl $^+$ cells possessed higher Glo-I protein levels than normal BM or PB cells (Supplementary Figure 5). These findings indicate that Glo-I expression was induced not only in the artificially generated HA-CML cell lines but also in primary Bcr-Abl $^+$ cells, suggesting that primary leukemic cells may be adapted to hypoxia *in vivo*.

High Glo-I expression is sustained in HA-CML cells after 6 months in normoxia. The HA cells returned to normoxic culture conditions revert to the parental cell proliferation rate after 5 days (Supplementary Figure 6a), and the fraction of cells in G_0 decreases within 48 h after return to normoxic conditions (Supplementary Figure 6b). Interestingly, the high level of Glo-1 expression developed by HA-CML cells was sustained after 6 months in culture under normoxic conditions (Supplementary Figure 6c).

Engraftment of HA-CML cells in NOG mice. We established stable subclones of K562 and K562/HA cells ($K562^{Luc\text{-}EGFP}$ and $K562/HA^{Luc\text{-}EGFP}$, respectively) that coexpressed luciferase and enhanced green fluorescent protein (EGFP). When we examined the bioluminescence of the cells, $K562^{Luc\text{-}EGFP}$ cells produced approximately 10 times more bioluminescence than did $K562/HA^{Luc\text{-}EGFP}$ cells (Figure 4a). As the strength of luciferase bioluminescence depends on the availability of ATP and oxygen, we hypothesized that these factors may have a role in the reduced bioluminescence of $K562/HA^{Luc\text{-}EGFP}$ cells. Engraftment and proliferation of $K562^{Luc\text{-}EGFP}$ and $K562/HA^{Luc\text{-}EGFP}$ cells in NOG mice were monitored using *in vivo* imaging (Figure 4a). Despite the lower level of bioluminescence in $K562/HA^{Luc\text{-}EGFP}$ cells in culture, there were no significant differences in total photon emission between $K562^{Luc\text{-}EGFP}$- and $K562/HA^{Luc\text{-}EGFP}$-engrafted mice before day 34. After day 34, the total photon emission of $K562/HA^{Luc\text{-}EGFP}$-engrafted mice increased much more sharply than that of $K562^{Luc\text{-}EGFP}$ mice (Figure 4b). In addition, $K562/HA^{Luc\text{-}EGFP}$-transplanted mice died significantly earlier than did $K562^{Luc\text{-}EGFP}$ mice (Figure 4c). These results indicate that $K562/HA^{Luc\text{-}EGFP}$ cells engrafted more efficiently in NOG mice than did the parental $K562^{Luc\text{-}EGFP}$ cells.

To investigate why $K562/HA^{Luc\text{-}EGFP}$ cells engrafted more efficiently, we examined the cell cycle distribution of K562 and K562/HA cells. The percentages of cells in G_0 in K562 and K562/HA cells were 0.87 + 0.58 and 4.9 + 2.1%, respectively, indicating that the K562/HA grafts included more quiescent cells than did the parental line (Figures 4d and e). Next, we examined the expression of c-kit, Tie-2, CXCR4, Notch, N-cadherin, VLA-4, LFA-1 and CD44, all of which have been reported to indicate stemness.[23] There was no difference in the expression levels of these proteins in K562/HA or KCL22/HA cells and the respective parental cell lines (data not shown). Interestingly, both HA cell lines expressed higher levels of β-catenin, which is thought to be important for

NPG.CDD.CDD20106

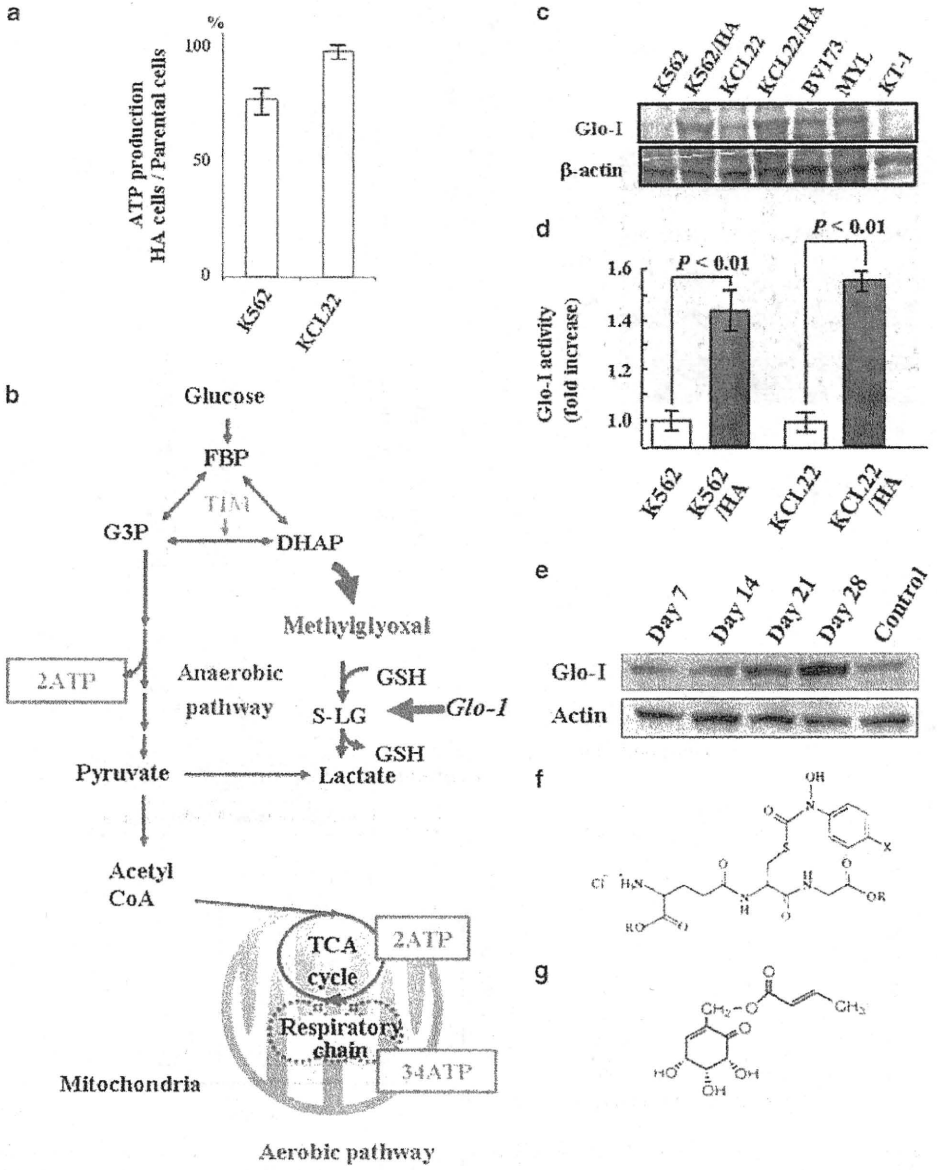

Figure 3 The influences of adaptation to hypoxia on ATP production and glyoxalase-I (Glo-I) activity. (**a**) ATP production is expressed as the ratio of production in hypoxia-adapted (HA) cells relative to parental chronic myeloid leukemia (CML) cells. (**b**) Schematic illustration of aerobic and anaerobic ATP production pathways. Methylglyoxal accumulates in cells that use the anaerobic pathway, and Glo-I functions to detoxify methylglyoxal. (**c**) Glo-I protein levels in parental CML cell lines and the respective HA subclones. (**d**) Glo-I activity in parental CML cell lines and the respective HA subclones. (**e**) Glo-I protein levels under hypoxic conditions. Glo-I expression was clearly evident 21 days after initiation of hypoxia (1.0% O_2). Chemical structures of *S-p*-bromobenzyl glutathione cyclopentyl diester (BBGC) (**f**) and 2-crotonyloxymethyl-4,5,6-trihydroxycylohex-2-enone (COTC) (**g**)

production of CML stem cells (Figure 4f).[24] In addition, the K562/HA cell line contained more cells with the side population marker for cancer stem cells (Figure 4g).[25] These findings suggest that the adaptation to hypoxia induces putative stem/progenitor cell-like characteristics in Bcr-Abl$^+$ cells.

Effect of Glo-I inhibitors on HA-CML cells. *S-p*-bromobenzyl glutathione cyclopentyl diester (BBGC) (Figure 3f) is a specific cell-permeable inhibitor of Glo-I,[26] and 2-crotonyloxymethyl-4,5,6-trihydroxycylohex-2-enone (COTC) (Figure 3g) is an inhibitor of Glo-I and glutathione.[27] Recently, methyl-gerfelin (Supplementary Figure 7a) was also identified as a Glo-I inhibitor.[28] Although HA-CML cells were resistant to the cytotoxic effects of Abl TKIs and alkylating agents (Figures 2d and e, Table 1), BBGC, COTC and methyl-gerfelin were more strongly cytotoxic in K562/HA and KCL22/HA cells than in the parental cell lines (Figures 5a–d, Supplementary Figures 7b and c).

To determine the mechanism of cell death induced by BBGC, we examined Annexin V staining (Supplementary

NPG.CDD.CDD20106